# Algorithm Theoretical Basis Document for the Cloud Mask of the NWC/PPS

NWC/CDOP2/PPS/SMHI/SCI/ATBD/1, Issue 1, Rev. 0

*15 September 2014*

## Applicable to SAFNWC/PPS version 2014

*Applicable to the following PGE:s:*

| PGE | Acronym | Product ID | Product name | Version number |
|---|---|---|---|---|
| PGE01 | CMa | NWC-062 | Cloud Mask | 4.0 |

**Prepared by Swedish Meteorological and Hydrological Institute (SMHI)**

**REPORT SIGNATURE TABLE**

| Function | Name | Signature | Date |
|---|---|---|---|
| **Prepared by** | SMHI | | 15 September 2014 |
| **Reviewed by** | SAFNWC Project Team<br><br>EUMETSAT | | <br><br>9 September 2014 |
| **Authorised by** | Anke Thoss, SMHI<br>*SAFNWC PPS Manager* | | 15 September 2014 |

# DOCUMENT CHANGE RECORD

| Version | Date | Pages | Changes |
|---|---|---|---|
| 1.0d | 22 January 2014 | 64 | Replacing CDOP-document: SAF/NWC/CDOP/SMHI-PPS/SCI/ATBD/1<br><br>First version for SAFNWC/PPS v2014<br><br>Changes since v2012:<br><br>-Updated according to scientific changes since v2012, se section 1.6<br><br>-Updated the output format.<br><br>-Some general update. |
| 1.0 | 15 September 2014 | 65 | Implemented RIDs from PCR-v2014:<br><br>-Act.4: Given a rational for using 6s and RTTOV.<br>-Act.7 Both operational and re-processed OSISAF ice maps can be used.<br>-DF1 (rewriting section 1.6)<br>-LSc1 (formal issues)<br>-LSc2 (summary of requirements)<br>-LSc3, PW1-PW7, PW10, PW12-PW19 (editorials and clarifications)<br>-PW8 (restructuring section 4.1.2)<br><br>Other changes:<br>-Updated the validation results, after v2014 final validation. |

# Table of Contents

# List of Tables and Figures

# 1. INTRODUCTION

The EUMETSAT "Satellite Application Facilities" (SAF) are dedicated centres of excellence for processing satellite data, and form an integral part of the distributed EUMETSAT Application Ground Segment ( http://www.eumetsat.int ). This documentation is provided by the SAF on Support to Nowcasting and Very Short Range Forecasting, SAFNWC. The main objective of SAFNWC is to provide, further develop and maintain software packages to be used for Nowcasting applications of operational meteorological satellite data by National Meteorological Services. More information can be found at the SAFNWC webpage, http://www.nwcsaf.org . This document is applicable to the SAFNWC processing package for polar orbiting meteorological satellites, SAFNWC/PPS, developed and maintained by SMHI ( http://nwcsaf.smhi.se ).

## 1.1 PURPOSE

This document is the Algorithm Theoretical Basis Document for the PGE01 (CMa, Cloud Mask) of the SAFNWC/PPS software package.

This document contains a description of the algorithm, including scientific aspects and practical considerations.

## 1.2 SCOPE

This document describes the algorithms implemented in the PGE01 version v4.0 of the 2014 SAFNWC/PPS software package delivery.

## 1.3 DEFINITIONS AND ACRONYMS

| Acronym | Explanation | Acronym | Explanation |
|---|---|---|---|
| **AAPP** | AVHRR and ATOVS Processing Package | **MAIA** | Mask Avhrr for Inversion Atovs (an AVHRR Cloud Mask) |
| **ACPG** | AVHRR/AMSU Cloud Product Generation software (A major part of the SAFNWC/PPS s.w., including the PGE:s.) | **MHS** | Microwave Humidity Sounding Unit |
| | | **NIR** | Near Infrared |
| **AEMET** | Agencia Estatal de Meteorología (Spain) | **NOAA** | National Oceanic and Atmospheric Administration |
| **AHAMAP** | AMSU-HIRS-AVHRR Mapping Library (A part of the SAFNWC/PPS s.w.) | **NWP** | Numerical Weather Prediction |
| | | **OSISAF** | Ocean and Sea Ice SAF |
| **AMSU** | Advance Microwave Sounding Unit | **PC** | Precipitating Cloud (also PGE04) |
| **AVHRR** | Advanced Very High Resolution Radiometer | **PGE** | Process Generating Element |
| | | **PPS** | Polar Platform System |
| **CDOP** | Continuous Development and Operational Phase | **RGB** | Red Green Blue |
| | | **RTM** | Radiative Transfer Model |
| **CDOP-2** | Second Continuous Development and Operational Phase | **SAF** | Satellite Application Facility |
| | | **SAFNWC** | Satellite Application Facility for support to NoWcasting |
| **CLAVR** | Clouds from AVHRR | | |
| **CMa** | Cloud Mask (also PGE01) | **SCANDIA** | Cloud Analysis model using digital AVHRR data |
| **CPP** | Cloud Physical Products | | |
| **CT** | Cloud Type (also PGE02) | **SMHI** | Swedish Meteorological and Hydrological Institute |
| **CTTH** | Cloud Top Temperature, Height and Pressure (also PGE03) | | |
| | | **SST** | Sea Surface Temperature |
| | | **TBC** | To Be Confirmed |
| **DEM** | Digital Elevation Model | **TBD** | To Be Defined |
| **EPS** | EUMETSAT Polar System | **TOA** | Top Of Atmosphere |
| **EUMETSAT** | European Organisation for the Exploitation of Meteorological Satellites | **USGS** | U.S. Geological Survey |
| | | **VIIRS** | Visible Infrared Imaging Radiometer Suite |
| **FOV** | Field Of View | **VIS** | Visible |
| **GEO** | Geosynchronus equatorial Orbit | | |
| **IR** | Infrared | | |
| **LEO** | Low Earth Orbit | | |

See [RD.1.] for a complete list of acronyms for the SAFNWC project.

## 1.4 REFERENCES

### 1.4.1 Applicable documents

The following documents, of the exact issue shown, form part of this document to the extent specified herein. Applicable documents are those referenced in the Contract or approved by the Approval Authority. They are referenced in this document in the form [AD.X]

For dated references, subsequent amendments to, or revisions of, any of these publications do not apply. For undated references, the current edition of the document referred applies.

Current documentation can be found at SAFNWC Helpdesk web: http://www.nwcsaf.org

| Ref | Title | Code | Vers | Date |
| --- | --- | --- | --- | --- |
| [AD.1.] | NWCSAF Project Plan | NWC/CDOP2/SAF/AEMET/MGT/PP | 1.2 | 28/06/13 |
| [AD.2.] | NWCSAF Product Requirements Document | NWC/CDOP2/SAF/AEMET/MGT/PRD | 1.5 | 05/06/14 |
| [AD.3.] | System and Components Requirements Document for the SAFNWC/PPS | NWC/CDOP2/PPS/SMHI/SW/SCRD | 1.0 | 15/09/14 |

*Table 1: List of Applicable Documents*

### 1.4.2 Reference documents

The reference documents contain useful information related to the subject of the project. These reference documents complement the applicable ones, and can be looked up to enhance the information included in this document if it is desired. They are referenced in this document in the form [RD.X]

For dated references, subsequent amendments to, or revisions of, any of these publications do not apply. For undated references, the current edition of the document referred applies

Current documentation can be found at SAFNWC Helpdesk web: http://www.nwcsaf.org

| Ref | Title | Code | Vers | Date |
| --- | --- | --- | --- | --- |
| [RD.1.] | The Nowcasting SAF Glossary | NWC/CDOP2/SAF/AEMET/MGT/GLO | 2.0 | 18/02/14 |
| [RD.2.] | User manual for the SAFNWC/PPS Application: Software Part, 2.Operation | NWC/CDOP2/PPS/SMHI/SW/UM/2 | 1.0 | 15/09/14 |
| [RD.3] | Validation Report for v.2014 of the SAFNWC/PPS | NWC/CDOP2/PPS/SMHI/SCI/VR/1 | 1.0 | 15/09/14 |
| [RD.4] | - | | | |
| [RD.5] | Output Data Format of the SAFNWC/PPS | NWC/CDOP2/PPS/SMHI/SW/DOF | 1.12 | 15/09/14 |

*Table 2: List of Referenced Documents*

### 1.4.3 Scientific References

Allen, R. C., Durkee, P. A., and Wash, C. H., 1990. Snow/cloud discrimination with multispectral satellite measurements. *Journal of Applied Meteorology* **29**, 994-1004.

Anderson, J., Hardy, E., Roach, J., and Witmer, R., 1976. A land use and land cover classification system for use with remote sensor data. Technical report, U.S. Geological Survey.

Berendes, T., Kuo, K., Logar, A., Corwin, E., Welch, R., Baum, B., Petre, A., and Weger, R., 1999. A comparison of paired histogram, maximum likelihood, class elimination, and neural network approaches for daylight global cloud classi_cation using AVHRR imagery. *Journal of Geophysical Research **104**(D6)*, 6199-6213.

Chevallier, F., Michele, S.D., and McNally, A.P., 2006. Diverse profile datasets from the ECMWF 91-level short-range forecast. *NWPSAF Research Report No. NWPSAF-EC-TR-010, 14p.*

Cox, C. and Munk, W., 1954. Measurement of the Roughness of the Sea Surface from Photographs of the Sun's Glitter. *Journal of the Optical Society of America **44**(11)*, 838-850.

Derrien, M., Farki, B., Harang, L., Gléau, H. L., Noyalet, A., Pochic, D., and Sairouni, A., 1993. Automatic cloud detection applied to NOAA-11/AVHRR imagery. *Remote Sensing of Environment **46***, 246-267.

Dybbroe, A., Karlsson, K.-G., and Thoss, A., 2005a. AVHRR cloud detection and analysis using dynamic thresholds and radiative transfer modelling - part one: Algorithm description. *Journal of Applied Meteorology **41**(1)*, 39-54.

Dybbroe, A., Karlsson, K.-G., and Thoss, A., 2005b. AVHRR cloud detection and analysis using dynamic thresholds and radiative transfer modelling - part two: Tuning and Validation. *Journal of Applied Meteorology **41**(1)*, 55-71.

Eidenshink, J. and Faundeen, J., 1994. The 1 km AVHRR global land data set-first stages in implementation. International Journal of Remote Sensing **15(17)**, 3443-3462.

Eyre, J. R., Brownscombe, J. L., and Allam, R. J., 1984. Detection of fog at night using Advanced Very High Resolution Radiometer (AVHRR) imagery. *Meteorological Magazine **113***, 266-271.

Hunt, G. E., 1973. Radiative properties of terrestrial clouds at visible and infra-red thermal wavelengths. *Quarterly Journal of the Royal Meteorological Society **99***, 346-369.

Inoue, T., 1985. On the temperature and effective emissivity determination of semi-transparent cirrus clouds by bi-spectral measurements in the 10 µm window region. Journal of the Meteorological Society of Japan **63(1)**, 88-98.

Karlsson, K.-G., 1996. Cloud Classification with the SCANDIA model. Reports Meteorology and Climatology **67**, SMHI.

Karlsson, K.-G. and Dybbroe, A., 2009. Evaluation of Arctic cloud products from the EUMETSAT Climate Monitoring Satellite Application Facility based on CALIPSO-CALIOP observations. *Atmos. Chem. Phys. Discuss., **9**, 16755-16810, 2009.*

Karlsson, K.-G., Rühelä A., Müller R., Meirink J.F., Sedlar J., Stengel M., Lockhoff M., Trentmann J., Kasper F., Hollmann R. and Wolters E., 2013. CLARA-A1: a cloud, albedo and radiation dataset from 28yr of global AVHRR data.. *Atmos. Chem. Phys. **13**,5351-5367, 2013 doi:10.5194/acp-13-5351-2013*

Karlsson, K.-G. and Johansson E, 2013, On the optimal method for evaluating cloud products from passive satellite imagery using CALIPSO-CALIOP data: example investigating the CM SAF CLARA-A1 dataset. *Atmos Meas. Thech. **6**, 1271-1286, 2013 doi:105194/amt-6-1271-2013*

Karlsson, K. and Dybbroe, A, 2010.: Evaluation of Arctic cloud products from the EUMETSAT Climate Monitoring Satellite Application Facility based on CALIPSO-CALIOP observations, Atmos. Chem. Phys, 10, 1789–1807..

Karlsson, K.-G. and Liljas, E., 1990. The SMHI model for cloud and precipitation analysis from multispectral AVHRR data. PROMIS reports **10**, SMHI. 74pp.

Seemann, S.W., E. E. Borbas, R. O. Knuteson, G. R. Stephenson, H.-L. Huang, 2007: Development of a Global Infrared Land Surface Emissivity Database for Application to Clear Sky Sounding Retrievals from Multi-spectral Satellite Radiance Measurements. *J. of Appl. Meteor. and Climatol.,* Vol. **47**, 108-123.

Salisbury, J. W. and d'Aria, D., 1994. Emissivity of terrestrial materials in the 3 - 5μm atmospheric window. *Remote Sensing of Environment 47*, 345-361.

Saunders, R. and Kriebel, T., 1988. An improved method for detecting clear sky and cloudy radiances from AVHRR data. *Int. J. Rem. Sens. 9*, 123-150.

Saunders, R., Matricardi, M., and Geer, A., 2008, RTTOV9.1 user guide, *UK Met office publication*, *NWPSAF-MO-UD-016*, 57p.

Stowe, L., McClain, E. P., Carey, R., Pellegrino, P., and Gutman, G. G., 1991. Global distribution of cloud cover derived from NOAA/AVHRR operational satellite data. *Adv. Space Res. 11*, 51-54.

Stowe, L. L., Davis, P. A., and McClain, E. P., 1999. Scientific Basis and Initial Evaluation of the CLAVR-1 Global Clear/Cloud Classification Algorithm for the Advanced Very High Resolution Radiometer. *Journal of Atmospheric and Oceanic Technology 16*, 656-681.

Vermote, E., Tanre, D., Deuze, J. L., Herman, M., and Morcrette, J. J., 1997. Second Simulation of the Satellite Signal in the Solar Spectrum: An overview, IEEE Trans. Geosci. Remote Sens., 35(3), 675-686.

Vermote, E., Tanre, D., Deuze, J. L., Herman, M., Morcrette, J. J., and Kotchenova, S. Y., 2006. Second Simulation of the Satellite Signal in the Solar Spectrum - Vector, 6S User Guide Version 3, http://www.6s.ltdri.org.

Warren, D., 1989. AVHRR channel-3 noise and methods for its removal. *International Journal of Remote Sensing 10*, 645-651.

## 1.5 DOCUMENT OVERVIEW

This document contains a theoretical description of the Cloud Mask algorithms. The document has been structured in the following sections:

Section 1 contains the current introduction along with the list of used acronyms and applicable and reference documents.

- Section 2 A short introduction to the cloud mask product

- Section 3 A short overview of the cloud mask algorithm

- Section 4 Algorithm description in more detail

## 1.6 SCIENTIFIC UPDATES SINCE PPS VERSION 2012

For v2014 PGE01 has been more harmonized in terms of output format and flags with the cloudmask product of GEO.

The following scientific changes have been made:

- Update of surface reflectivity treatment over land to improve cloud mask quality:

  o the threshold-tables for land-day scheme, where the 3.7µm channel is involved, have been revised. Here the solar contribution is now considered explicitly based on 6S radiative transfer calculations. To include solar contribution, a new, more complex threshold table structure had to be implemented

- Revision and tuning of cloud mask sub schemes (depending on context and illumination) based on sub-scheme performance as evaluated against CALIPSO data and from visual inspection of problem cases.

  o The test-logic has been cleaned and restructured where necessary.

  o Introduction of some new cloud screening tests under specific conditions.

  o A thorough retuning of threshold offsets has been performed.

- A new set of clear screening tests have been implemented

  o Improved treatment of cloud mask over water bodies when their extent differs between reality and land/sea mask

  o Restoral of certain heavy aerosol cases (dust) to cloud free and adding of respective processing flag

  o Test for very cold clear areas

- Roughness is used instead of high terrain as indication of mountain

- Updated emissivity maps.

# 2. INTRODUCTION TO THE SAFNWC/PPS CLOUD MASK

The Cloud Mask is the most basic product of the Polar Platform System (PPS) based cloud and precipitation products and necessary for the production of the other cloud and precipitation products. The aim of the Cloud Mask product is to delineate all absolutely cloud-free pixels in a satellite scene with high confidence. In addition, it will identify cloud free snow or ice contaminated pixels when illumination allows and provides processing flags indicating processing conditions and estimated quality for each pixel. The Cloud mask can thus be used both as input to products which will require information on cloud free pixels for further processing, and as input to a more detailed cloud analysis.

The SAFNWC/PPS have been developed for the Advanced Very High Resolution Radiometer (AVHRR) onboard the polar-orbiting weather satellites NOAA and Metop. It has been implemented so that it automatically handles both AVHRR/2 data, with channel 3B during both day and night, and AVHRR/3 data, with channel 3B during night and 3A during day. The instrument measures outgoing reflected solar energy and radiated thermal energy from land, sea, clouds and the atmosphere in 6 channels. As the AVHRR channels have different sensitivity from those different features, the SAFNWC/PPS algorithm uses this for its product derivation.

The SAFNWC/PPS has also been adapted for the Visible Infrared Imaging Radiometer Suite (VIIRS) onboard the polar-orbiting weather satellite NPP, and the coming JPSS satellites. The VIIRS channels used are the channels corresponding to the AVHRR channels, with an addition of the channel 8.5μm.

The actual PPS software has its roots in the older SCANDIA algorithm (Karlsson and Liljas, 1990 and Karlsson, 1996). This scheme has several similarities to other approaches of that era (e.g. APOLLO [Saunders and Kriebel, 1988], LUX [Derrien et al., 1993] and CLAVR [Stowe et al., 1991 and Stowe et al., 1999]). Common is the use of the typical differences in cloud appearances in all five spectral channels of the AVHRR instrument by applying sequences of threshold tests. However, a common weakness is that these earlier schemes employ static or partially static thresholds which are regionally specific. In some cases thresholds depend on season or the sun elevation according to a few classes, but no dynamic adaptation is made to the actual state of the atmosphere and surface at each individual field of view (FOV), and no consistent correction for the sun satellite viewing geometry is made. In the development and design of the new SAF retrievals for cloud mask analysis and cloud type classification three things have been of particular importance. First we wanted to improve corrections for bi-directional and atmospheric effects. Second, wherever possible, dynamic thresholds depending on the current atmospheric state, the actual illumination, viewing conditions and the state of the surface at the satellite footprint, are used, rather than static climatologically determined thresholds. Finally it should be possible to adapt the algorithms in a consistent way to future AVHRR and sensors with AVHRR heritage channels (e.g. MODIS or JPSS).

The way in which we have chosen to meet these requirements is to use radiative transfer models (RTMs) to simulate the satellite signal as it would have been observed in cloud free but otherwise similar conditions.

## 2.1  Satellite channels

Satellite channels used by the SAFNWC/PPS are from the Metop and NOAA imager instrument AVHRR/3 as well as from MODIS and VIIRS. See Table 3, Table 4 and Table 5 for more details about the different channels.

*Table 3: The AVHRR/3 channels and their approximate spectral positions on NOAA 15, 16 and 17 (small deviations in the spectral response do occur between individual instruments on different NOAA satellites).*

|          | Ch 1      | Ch 2      | Ch 3A     | Ch 3B     | Ch 4      | Ch 5      |
|----------|-----------|-----------|-----------|-----------|-----------|-----------|
| λ (µm)   | 0.58-0.68 | 0.725-1.0 | 1.58-1.64 | 3.55-3.93 | 10.3-11.3 | 11.5-12.5 |

*Table 4: Names and spectral specifications of MODIS channels, used so far. Channel 29 has no complement on any AVHRR instrument and is introduced here as an extension.*

|          | Ch 1      | Ch 2            | Ch 6            | Ch 20     | Ch 29   | Ch 31          | Ch 32           |
|----------|-----------|-----------------|-----------------|-----------|---------|----------------|-----------------|
| λ (µm)   | 0.62-0.67 | 0.841-<br>0.876 | 1.628-<br>1.652 | 3.66-3.84 | 8.4-8.7 | 10.78-<br>11.28 | 11.77-<br>12.27 |

*Table 5: Names and spectral specifications of VIIRS channels, used so far.With the exception minor differences in spectral response functions,  the VIIRS channels are similar to those used for MODIS..*

|          | Ch M5  | Ch M7 | Ch M10 | Ch M12 | Ch M14 | Ch M15 | Ch M16 |
|----------|--------|-------|--------|--------|--------|--------|--------|
| λ (µm)   | 0.672  | 0.865 | 1.61   | 3.7    | 8.55   | 10.763 | 12.013 |

### 2.1.1  Solar channels

Because of their different names that come with different instruments, channels are determined by their spectral position rather than by their name. Exceptions are made in case of referencing to instrument- specific issues.

In the 0.6µm channel, clouds appear bright because of the high reflectance while the signal from land and sea is generally poor (exception: sunglint areas over sea). Snow and ice on ground also appear bright. For the 0.8µm channel, the contrast between clouds and land is high and reflectance from sea surface is low, too (except for sunglint areas). However the signal from vegetated land is more intense compared to the 0.6µm channel.

The 1.6µm channel, is a so called near IR-channel. It allows to distinguish between snow/ice covered land and signal from other sources. The reflectance from snow and ice decreases with increasing wavelength in the Visible to NIR spectral range, and the reflectance over snow/ice is thus much smaller than in the 0.6µm or 0.8µm channels, providing a means to detect snow cover on the ground during daytime. Similarly this channel is also sensitive to the cloud phase; water clouds reflect more energy in this spectral range than ice clouds.

### 2.1.2 Thermal channels

The 3.7µm channel, lies in the spectrum where the outgoing energy comes from two sources: solar reflectance and thermally emitted radiation. This channel is sensitive to cloud phase and is particularly useful for the detection of night-time water clouds. The detection of thin cirrus can be done by analysing differences of the 3.7µm channel to the 11µm or the 12µm channel. Snow-covered ground has almost no contribution to the signal, received within this spectral range.

In the region around 8.5µm, there is a channel (unfortunately not on AVHRR instruments) close to one ozone-line but still in the window region. This channel in combination with the 11µm channel has a pronounced strength in detecting low clouds over certain surfaces (e.g. woodlands) under large observation angles. Additionally it might enhance the contrast in the night cirrus test if used instead of one of the 11 or 12 micron channels.

The channel, located round11 µm, is what is often referred to as the "IR window channel", i.e. radiation from the Earth's surface or cloud tops is little effected by extinction in the atmosphere. This channel responds to the temperature of clouds and surfaces and returns a signal close to what is called the thermodynamic temperature. The characteristic of the 12µm channel is very similar to its neighbour at 11µm. However, there are some differences, for example the detection of cirrus (the atmosphere seems denser with increasing wavelength).

## 2.2 REQUIREMENTS

The requirements for the SAFNWC/PPS products are described in the Product Requirements Document [AD.2.]. In Table 6 is given a summary of the requirement specific for the cloud mask product.

*Table 6 Accuracy requirements for Cloud Mask*

| | **POD (Europe)** | **FAR (Europe)** | **POD (global)** | **FAR (global)** |
| --- | --- | --- | --- | --- |
| **Threshold accuracy** | 85% | 20% | 85% | 20% |
| **Target accuracy** | 95% | 10% | 90% | 15% |
| **Optimal accuracy** | 98% | 5% | 95% | 10% |

# 3. ALGORITHM OVERVIEW

The CMa algorithm is based on a multi-spectral threshold technique applied to each pixel of the satellite scene. As in the SCANDIA model the threshold tests of the SAF CMa algorithm are coupled or grouped together, so that the identification of a cloud-filled or cloud-contaminated pixel requires that several threshold tests (one for each applicable image feature) all must be passed.

For every satellite scene a unique set of feature thresholds is extracted in full image resolution and applicable only for that particular composition of instrument, surface conditions and atmospheric conditions. The features employed are listed in Table 7. The thresholds applied to the spectral features *R0.6*, *T11*, *T11T3.7*, *T11T12*, *T3.7T12*, T85T11, and *T11Tsur* are what we call dynamic and have all been derived by calculating the cloud free satellite signal using RTM simulations. For the simulations of thermal radiation and brightness temperature, the model RTTOV9 (Saunders et al., 2008) is used. Simulations of solar radiances and reflectances are performed with the Second Simulation of a Satellite Signal in the Solar Spectrum (6S; Vermote et al., 1997, 2006). Even though these simulations (infra red and solar) are done offline, calculation speed is an issue. In the solar part 5103 tables (each with 10000 profiles) have to be prepared for proper statistics. The selected models fulfil the minimum requirements (in terms of optical and geometrical properties), are well established in the community and are reasonable fast.

Resulting radiances (for the 3.7µm channel a combination of solar and thermal contribution) are a function of the actual atmospheric state, the surface characteristics, and the sun-satellite (for pure IR channels just the satellite) viewing geometry. The lack of both a sufficiently reliable global land-use database and accurate surface BRDF's (Bidirectional Reflectance Distribution Functions), together with uncertainties in geo-location (this problem appears mainly for the AVHRR instrument), the high anisotropic behaviour of earth surfaces and the high pixel to pixel variability of the reflectance at 1.6 and 3.7µm, prevented us so far from trying to simulate the TOA signals at these wavelengths. For version 2014, however, we included the solar component of the 3.7µm channel in the threshold-tables for daytime use over land. Reflection is assumed to follow the lambertian description. This makes the results more robust against uncertainties in land surface characterization and inhomogeneities within satellite pixels. Improvements due to the new, more complete threshold tables are most pronounced for semi-arid areas which possess a relatively low emissivity and therefore, following Kirchoffs law, a higher reflectivity in this spectral region. For a detailed description of the derivation of the dynamic thresholds please refer to Dybbroe et al., 2005a.

The dynamic thresholds are determined from satellite dependent look-up tables (stored in ASCII or HDF5 format). The pure IR tables are multidimensional, depending on viewing geometry (satellite viewing angles), NWP parameters (surface temperature and total water vapour column) and surface emissivity. IR-threshold-tables over land are calculated for an emissivity of 0.8 (= ε ref) on the base of 10000 atmospheric profiles. These thresholds are corrected according to actual or climatological emissivity-maps afterwards. Therefore gain and intercept matrices (with the same rank as referring thresholds) are calculated, determine the change of threshold value with change of emissivity for all atmospheric and surface conditions:

The slope for the *i*:th profile is given by

$$a_i = \frac{TB_i(\varepsilon \equiv 1.0) - TB_i(\varepsilon \equiv 0.6)}{0.4}$$

This leads to a mean slope

$$\overline{a} = \frac{1}{N} \sum_{i=1}^{N} a_i$$

And to a mean intercept as

$$\overline{b} = -\overline{a}\,\varepsilon_{ref}$$

Since the relationship between emissivity and brightness temperature for cloudfree atmospheres is sufficient linear on small scales, the threshold values are corrected by shifting them along the calculated functions. As mentioned above an exception is made during daytime and in case the 3.7µm channel is involved in calculating the feature. Here solar and thermal contributions are calculated independently and merged later. The explicit simulation of the solar share involves a more complex structure of threshold tables. Additionally to the above parameters, these merged (feature solar and thermal contributions) thresholds are dependent on solar zenith angle, aerosol load and model (right now only the low amount of a typical maritime scenario is used), and surface reflectivity. The reflectivity is derived directly from the 3.7µm emissivity maps.

The thresholds are computed in full resolution as dictated by the defined processing region (see [RD.2.]). Constant offsets to the dynamic thresholds, determined during algorithm tuning, are also often applied. See (Dybbroe et al., 2005b) for details on algorithm tuning. Different offsets may be applied over sea, sea ice and land, and dependent on the illumination (day, night or twilight). In addition to these dynamic thresholds also constant, or linearly (e.g. in the sun zenith angle) varying thresholds determined empirically, are applied. Coefficients determining these are available in a static ASCII file (threshold_offsets.cfg, and threshold_offsets_gac.cfg for GAC-settings), which is not normally to be altered by the user.

The thresholding is fuzzy in the sense that the distances in feature space to the thresholds are stored and used to determine whether to stop or continue testing, this is also used as a quality indicator of the final output. More details are provided in section 4.1.2.10 After the thresholding a filtering is applied. In this post-processing all isolated pixels of which classification is based on the 3.7µm channel are reclassified to be equal to its neighbours. This is done in order to correct artificial results due to unsettle 3.7µm signal to noise ratio.

# 4. ALGORITHM DESCRIPTION

# 4.1 THEORETICAL DESCRIPTION

### 4.1.1 Physics of the Problem

Light entering the detector onboard a satellite platform carries somehow information on interactions with matter on its path with it. The task addressed to an inverse algorithm, is to use this information to retrieve the nature of the matter that caused it.

In order to derive a cloudmask, the complexity reduces to the question whether a pixel is cloudy or not. The approach chosen here to solve this problem is a threshold technique. A pixel is considered cloudy if the measured reflectance or brightness-temperature deviates in a certain way from pre-calculated clear-sky values.

Since there is more matter around than just clouds that may affect a pencil of rays, it is necessary to reduce these perturbances as far as possible. The moving positions of sun and satellite are also sources of perturbing variations within the received signal. To account for this uncertainty, dynamical thresholds are used (i.e. thresholds are not fixed but adapted to atmospheric, surface, and geometrical conditions).

Generally, most of cloudy pixels can be detected because of a lower temperature (observed at 10.8 µm) or a higher reflectivity (in the solar wavelengths at 0.6 and 0.8 µm) compared to their cloud-free counterparts. Obviously this doesn't hold for all cases (e.g. over cold surfaces, for low clouds, over desert areas, etc.) therefore several independent informations have to be taken into account to determine the cloud-status and to address the quality of the product. This is done by combining observations at different wavelengths with informations on the spatial structure.

### 4.1.2 Mathematical Description of the Problem

#### 4.1.2.1 Features

Table 7 shows the utilised image features for all channels. Note that not all channels are provided by all instruments (e.g. no 8.5um channel on AVHRR instruments). As seen from the table we use both spectral features and local texture (spatial variability) features. The spectral features are both simple linear combinations (differences) of channel reflectances or brightness temperatures and non-linear features such as the ratios of the 1.6µm and 3.7µm over the 0.6µm reflectance. One spectral feature is the difference between the T11 and the forecasted thermodynamic skin temperature. This is the only feature making direct use of non-satellite data (but other features are indirect dependent on NWP data). The texture features are all derived by taking the standard deviation of a spectral feature over a 5 by 5 (or 3 by 3) pixel size box centred on the given pixel. For GAC settings a 3 by 3 pixel size box is used, for not-GAC settings a 5 by 5 pixel size box is used. This distinction is because the original GAC-pixels are bigger, and a 5 by 5 pixel box is getting too big then.

The feature creation and selection has been done to a large extent following past experience with thresholding AVHRR data for cloud classification, as in e.g SCANDIA, APOLLO, LUX, and CLAVR. But, there are a number of new features as compared to these known cloud schemes. One

example is the texture feature derived from the local standard deviation of the brightness temperature difference between 3.7µm and 12 µm motivated later.

There is of course a significant amount of redundant information in this large set of features used. The dimension of the feature space described by the 16 selected features is not 16, but rather somewhat smaller, and many of the features are strongly dependent on each other. A principal component analysis using a hypothetical large amount of training data might show that the features chosen are not optimal for the description of the feature space. However, for our purpose it has been important to select features for which it is possible to reason in a consistent physical manner on how they may be affected when clouds with different physical characteristics (in terms of particle size, shape, and phase distribution) fill the FOV.

In the subsections below we give a short summary explanation and motivation for the chosen image features listed in Table 7. More physical explanations and how the features are applied can be found in Table 9, Table 10, Table 11, Table 12 and Table 13.

*Table 7: List of utilised image features (Note: Not all listed features are provided by all instruments).*

| Image feature | Composition |
|---|---|
| R0.6 | Reflectance for 0.6µm channel |
| PseudoR0.6 | Reflectance assuming sun in zenith for 0.6µm channel |
| R0.6_text | Local (5 by 5 pixels, 3 by 3 for gac) R0.6 standard deviation |
| R1.6 | Reflectance for 1.6µm channel |
| R3.7 | Reflectance for 3.7µm channel (derived from T3.7 subtracting the thermal part using T11) |
| QR1.6R0.6 | Reflectance ratio of R1.6 and R0.6 |
| QR0.9R0.6 | Reflectance ratio of R0.9 and R0.6 |
| QR3.7R0.6 | Reflectance ratio of R3.7 and R0.6 |
| T11 | Brightness temperature for 11µm channel |
| T11T3.7 | Brightness temperature difference of 11 and 3.7µm channels |
| T11_text | Local (5 by 5 pixels, 3 by 3 for gac) T11 standard deviation |
| T11T12 | Brightness temperature difference of 11 and 12µm channels |
| T3.7T12 | Brightness temperature difference of 3.7 and 12µm channels |
| T3.7T12_text | Local (5 by 5 pixels, 3 by 3 for gac) T3.7T12 standard deviation |
| T37_text | Local (5 by 5 pixels, 3 by 3 for gac) T3.7 standard deviation |

| Image feature | Composition |
|---|---|
| **T11Tsur** | **Difference between T11 and forecasted surface temperature** |
| **T85T11** | **Brightness temperature difference between 8.5 and 11µm channel** |

### 4.1.2.1.1 Feature R0.6

The reflectance at 0.6µm is used to distinguish clouds and snow from a dark background (snow-free and cloud-free land or ocean surface, see Table 8,Table 9 and Table 10) when the sun is significantly above the horizon. The sun elevation limit is set to 4º. For the separation of cloudy and cloudfree snow covered surfaces features using the near infrared or thermal infrared channels at 1.6 and 3.7µm must be used (see later). This feature is tested using a dynamic threshold. However, knowing the difficulties in simulating realistically the top of atmosphere (TOA) reflectance, due to BRDF deficiencies and lack of knowledge about the actual state of the surface, we use this feature both over land and over sea only with rather conservative threshold settings, that is with threshold values far from the average (or normal) cloudfree values.

Thus, away from snow covered areas this feature, if applied alone, would most often fail to detect both water clouds only filling the FOV partially and thin cirrus clouds. But being a grouped thresholding algorithm this feature is always applied together with other tests as seen from Table 12.

### 4.1.2.1.2 Feature PseudoR0.6

The reflectance at 0.6µm assuming sun in zenith (i.e. not applying the correction factor $1/\cos(\Theta sun)$) is used to distinguish clouds and snow from a dark background at low sun elevations ($< 4º$). (See Table 11). This feature is tested against an empirically derived threshold linearly dependent on the sun elevation.

This feature is introduced in order to attempt utilising fundamental reflection differences (e.g. between snow/clouds and snow-free/cloudfree surfaces) even at very low sun elevations. The feature is especially important in cases when a pixel exhibits illumination and the 1.6µm channel is still not switched on, as the 3.7µm channel signal gets highly ambiguous at very low sun elevations.

### 4.1.2.1.3 Feature R1.6

The reflectance at 1.6µm is particular useful in the detection of low water clouds over snow covered surfaces (over land and sea-ice) and in sunglint areas over water bodies.

### 4.1.2.1.4 Feature R3.7

The reflectance at 3.7µm is derived by subtracting the emission part from the 3.7µm radiance using 11µm channel under the assumption of unit emissivity (see Allen et al. (1990) for a derivation). As above, this feature is particular important when attempting to detect low water clouds over either snow covered surfaces (over land and sea-ice) or water bodies in sunglint.

### 4.1.2.1.5 Feature QR1.6R0.6

The reflectance ratio between R1.6 and R0.6 is used in particular in the separation of water clouds from snow cover (over land and sea-ice) and sunglint.

### 4.1.2.1.6 Feature QR3.7R0.6

The reflectance ratio between R3.7 and R0.6 is used in particular in the separation of water clouds from snow cover (over land and sea-ice) and sunglint.

### 4.1.2.1.7 Feature QR0.9R0.6

The reflectance ratio between R09 and R06 was introduced in beginning of 2006 as a result of an inter-comparison study between the MAIA and the PPS cloud mask schemes, in particular over the arctic. There it was found that in particular when having no 3.7µm channel (but 1.6µm channel) the low cloud detection in sunglint with the feature QR1.6R0.6 was not as efficient as expected, and that this additional feature might help. Also, in more recent updates to PPS, this feature is used more frequently, for instance in the new clear tests which try to account for the, mainly man-made impacted, varying land use with time. See 4.1.2.8.

### 4.1.2.1.8 Feature T11

The 11µm brightness temperature is used to detect cold clouds. It is normally used with a rather high offset to avoid miss-classifying cold land surfaces as clouds, and it is only used alone when all other usual low cloud features fail (during twilight and in cases of super-cooled water particles during night).

### 4.1.2.1.9 Feature T11T3.7

The brightness temperature difference between the 11µm and 3.7µm channels is used to detect water clouds at night. This is a well known technique to detect stratus and fog at night as e.g. used by Eyre et al. (1984) using the findings of Hunt (1973).

### 4.1.2.1.10 T11_text

The local texture in the 11µm brightness temperature is used to detect sub-pixel clouds and cloud edges over sea, and requires a cloud top temperature different (warmer or colder) from the surface in order to be effective. This feature is always applied together with other texture features, in order to avoid miss-classifying pixels in sea surface temperature gradient zones as being cloud contaminated.

### 4.1.2.1.11 Feature T11T12

The brightness temperature difference between 11 and 12µm channel is used for thin cirrus detection due to the decrease of transmisivity of these clouds with increasing wavelength (Inoue, 1985). Its main use is during daytime, as it can be replaced by the T3.7T12 (see below) during night. If the 8.5µm channel is available, a combination with the 11 or 12µm channel will merge advantages of both mentioned tests: It will provide a better contrast than the T11T12 feature and is not affected by solar radiation during daytime like the T3.7T12 feature.

Over sea ice we use this feature during night-time to detect transparent clouds that are warmer then the underlying surface. Here the 11µm 12µm channel difference is often negative.

### 4.1.2.1.12  Feature T3.7T12

The brightness temperature difference between 3.7µm and 12µm channel, is similar to the above feature, and is used to detect thin cirrus. The feature is more sensitive to thin cirrus and has proven useful on the later NOAA (15 and later) satellites where the earlier observed periodic noise (Warren, 1989) seems to have disappeared.

### 4.1.2.1.13  Feature T3.7T12_text

The local texture in the 3.7µm and 12µm channel brightness temperature difference is used together with T11_text to detect sub-pixel clouds and cloud edges. Due to the strong non linearity of the Planck function at 3.7µm the brightness temperature difference has a significant non-linear response to the fractional cloud cover over the satellite FOV. Assuming a cloud top temperature different from the surface, a partially covered pixel will have a large brightness temperature difference, compared to its cloud free or completely cloud covered neighbour (over the sea). This assumes that any co-located sea surface temperature gradient is smoother than the cloud/no cloud boundary which is under detection.

In addition, this feature has been proven to be powerful to filter channel 3b noise. With the new AVHRR sensor, ch3b noise is only a problem at very low temperatures and this feature is thus only applied over sea ice during night-time.

### 4.1.2.1.14  Feature T3.7_text

The T3.7_text feature is only used over sea ice during night-time. Sea ice surfaces often contain leads (= cracks filled with water) which are of sub-pixel size. The T3.7_text feature can filter these leads.

### 4.1.2.1.15  Feature T11Tsur

This feature describes the difference between the measured brightness temperature at 11µm and an assumed surface skin temperature (in our case described by a short range NWP model forecast). In the Arctic we apply this feature to detect clouds that are significant warmer then the underlying surface.

### 4.1.2.1.16  Feature T85T11

Similarly to the T11T12 and the T37T12 features this feature is meant to detect thin cirrus. Even if it is less sensitive than the T37T12 feature it has the advantage that it can be used during daytime without introducing any uncertainty due to daylight. On the other hand it is expected to be more sensitive than the T11T12 feature which also works fine during daytime.

## 4.1.2.2  Threshold Tests

### 4.1.2.2.1  Threshold tests, per function

*Table 8: Clear tests used to screen out obvious clear pixels before the cloud tests.*

| Component name (and result) | Used image features | Function |
| --- | --- | --- |
| **Clear New Water Bodies**<br><br>**(Cloudfree)** | QR0.9R0.6<br><br>R0.6<br><br>T3.7T12<br><br>T3.7T11 | **Test for clear water bodies not included in PPS landuse. Used during daytime over land (coast).** |
| **coldClearArcticAreaTest**<br><br>**(Cloudfree)** | T11Ts<br><br>Tsur<br><br>T11T12<br><br>(T11T3.7) | **Test for cold clear arctic (very cold) areas. Test will pass if: T11 –T12 is reasonable for clear conditions, T11 is close to forecasted surface temperature, temperature is below 230K and T11-T37 need to be within reasonable clear conditions if ch 3.7 is available. In very cold regions channel 3.7 is often nodata. Test is used during night and twilight over land (coast)** |
| **SaltLakeTest**<br><br>**(Cloudfree)** | QR0.9R0.6<br><br>R0.6<br><br>T11<br><br>T11Tsur<br><br>T3.7T12<br><br>T11T12 | **Test is used during day over sea (coast). The aim is to catch obvious cloudfree pixels over areas that are open water according to the USGS land use database, but where a high reflectivity indicates a dried out lake or salt lake. If not catched early such a dry or semi-dry salt lake will always be classified cloudy in daytime.**<br><br>**This test requires the 3.7 micron channel.** |
| **DriedOutLakesAndRiversTest**<br><br>**(Cloudfree)** | QR0.9R0.6<br><br>T11<br><br>T11Tsur<br><br>T11T12<br><br>(T3.7T12) | **Test is used during day over sea (coast). Similar to the above test, but 3.7 micron channel is not mandatory. Thus this test is active on Metop/AVHRR data (where only the 1.6 micron channels is available).** |

| Component name (and result) | Used image features | Function |
|---|---|---|
| **Not Cloud Heavy Aerosols** **(Cloudfree)** | R0.6 T11Tsur T11T12 T3.7T12 | **Test for heavy aerosols which is not clouds.** **This test will pass for pixels that have low reflectivity in channel 0.6, T11 –T12 is within reasonable margins for clear and we have a very large channel T37-T12 difference. Test is used during day over land.** |

*Table 9: The components (generic tests) of the grouped threshold tests applied in the snow screening using the 3.7µm channel.*

| Component name (and result) | Used image features | Function |
|---|---|---|
| **Snow/Ice Sea and Snow/Ice Sea Ice** **(Snow/Ice contaminated)** | T11Tsur T11 R3.7 R0.6 QR3.7R0.6 T3.7T12 T11T12 | **Detects snow covered sea ice or old sea ice during day and twilight. The T11 has to be close to the forecasted surface temperature but colder than 278K. The channel 3B reflectance shall be smaller than 10%. To avoid thin cirrus (over open sea) to be erroneously detected as snow the R0.6 shall be sufficiently large, the ratio R3.7/R0.6 small and T3.7T12 small (< 5K). To avoid misclassifying opaque clouds T11T12 shall be bigger than the cloud-free value minus 1K. The T3.7T12, QR3.7R0.6 and R3.7 features are combined with OR statements and rather conservative threshold settings are applied. We have seen that the information content of this features is complementary.** |
| **Snow Land** **(Snow/Ice contaminated)** | T11 R3.7 R0.6 QR3.7R0.6 T3.7T12 T11T12 (T11Tsur) | **Detects snow cover during day and twilight over land surface and in coastal regions. Equal to the previous test, except for two features: The T11Tsur is used only in case where no low level temperature inversions are present. Furthermore to avoid mis-classifying shadows on clouds (something which is particular a problem when not using the T11Tsur) the T3.7T12 is not allowed to be too small (> 0.5K).** |

| Component name (and result) | Used image features | Function |
|---|---|---|
| **Snow Sunglint** <br><br> **(snow/Ice contaminated)** | T11 <br><br> R3.7 <br><br> R0.6 <br><br> QR3.7R0.6 <br><br> T3.7T12 <br><br> (T11Tsur) | **Detects snow cover during day and twilight over sea, coast and land surfaces in potential sunglint areas. Except for the T11T12 feature, which is not used here and a higher tolerance in T3.7T12 (< 10K) due to increased forward scattering, the test is equal to the one above.** |
| **Snow Mountain** <br><br> **(Snow/Ice contaminated)** | T11 <br><br> R3.7 <br><br> R0.6 <br><br> QR3.7R0.6 <br><br> T11Tsur | **Detects snow cover during day and twilight (at sun elevations higher than 4º) over elevated terrain (> 500m) over land and coast. Similar to the previous test. The T11Tsur is used with a more conservative threshold offset due to the higher uncertainty of the forecasted surface temperature in highly variable terrain. Also no tests using T11T12 and T3.7T12 are performed here as rough topography may give highly non-uniform FOV in these features, known to raise the values in these features.** |
| **Snow Twilight** <br><br> **(Snow/Ice contaminated)** | T11 <br><br> PseudoR0.6 <br><br> R0.6 <br><br> T3.7T12 <br><br> (T11Tsur) | **Detects snow cover during twilight over land and in coastal areas. When the sun is below the horizon (sun zenith > 90º), the PseudoR0.6 has to be greater than 1.5%. When the sun is above the horizon this threshold increases linearly with increasing sun elevation with a gain of 0.5%/degree. The remaining feature tests are as in the Snow/Land test.** |

*Table 10: The components of the grouped threshold tests applied in the snow screening using the 1.6μm channel.*

| Component name (and result) | Used image features | Function |
|---|---|---|
| **Snow Sea / Sea Ice 3A** <br><br> **(Snow/Ice** | T11Tsur <br><br> T11 <br><br> R0.6 | **Detects snow covered sea ice or cold sea ice during day and twilight. The T11 has to be close to the forecasted surface temperature but colder than 278K. To avoid thin cirrus (over open sea) to be erroneously interpreted as snow the R0.6 shall** |

| Component name (and result) | Used image features | Function |
| --- | --- | --- |
| contaminated) | QR1.6R0.6<br><br>T11T12 | **be sufficiently large, the ratio R1.6/R0.6 small and T11T12 is not allowed to be too small. It shall be smaller than minus 1K plus the dynamic cloud threshold.** |
| **Snow Sea / Sea Ice 3A v2014**<br><br>**(Snow/Ice contaminated)** | T11Tsur<br><br>T11<br><br>R0.6<br><br>QR1.6R0.6<br><br>T11T12 | **The previous snow-seaice test for the 1.6 micron channel over sea had typical problems over smaller water bodies where the NWP t-skin can be off by 10-15 K and even more, especially in the spring season when the surrounding land warms up considerably after sunrise. This new test relaxes the t11-tsur threshold depending on the strength of the snow signal in the VIS/NIR channels.**<br><br>**The departure of the observation in three image features to the expected cloudfree and snow covered values is estimated. The features are T11-T12, R06, and the reflectance quota QR1.6R0.6. The departures are then multiplied to give an offset to be applied to the T11Tsur test, so that a large overall departure (in 3d space) requires the T11 to be much colder than the predicted cloudfree surface skin temperature.** |
| **Snow Land 3A**<br><br>**(Snow/Ice contaminated)** | (T11Tsur)<br><br>T11<br><br>R0.6<br><br>QR1.6R0.6<br><br>R1.6<br><br>T11T12 | **Detects snow cover over land and coast during day and twilight. Same as the previous test except for three of the feature tests. The T11Tsur is used only in cases where no low level temperature inversion is present. The T11T12 is not bounded on the low side and it is allowed to be 1.5K higher than the dynamic cloudfree threshold. The R1.6 not used above is used here with an empirically determined threshold varying linearly on the secant of the satellite zenith angle – one for the forward scattering mode and another for the backward scattering mode. (The forward scattering is allowed to be larger than the backward scattering).** |
| **Snow Sunglint 3A**<br><br>**(Snow/Ice contaminated)** | T11<br><br>R0.6<br><br>QR1.6R0.6<br><br>(T11Tsur) | **Detects snow cover during day and twilight over sea, coast and land surfaces in potential sunglint areas. The thresholds in T11, R0.6 and T11Tsur are the same as those used in the corresponding AVHRR/2 tests with channel 3B. The R1.6/R0.6 feature is thresholded as in the test above.** |

| Component name (and result) | Used image features | Function |
|---|---|---|
| **Snow Mountain 3A** <br> **(Snow/Ice contaminated)** | T11 <br><br> R0.6 <br><br> QR1.6R0.6 <br><br> T11T12 | **Detects snow cover during day and twilight (at sun elevations higher than 4º) over elevated terrain (> 500m) over land and coast. Similar to the Snow Land 3A test above, except that no testing is performed using T11Tsur. This due to the higher uncertainty in the forecasted surface temperature in highly variable terrain.** <br><br> **There is a slight inconsistency in the use of feature T11T12 and T11Tsur (see Table 9) respectively. This discrepancy has grown historically and does not do any harm to the products.** |
| **Snow Twilight 3A** | **PseudoR0.6** <br><br> **T11** <br><br> **R0.6** <br><br> **QR1.6R0.6** <br><br> **T11T12** <br><br> **(T11Tsur)** | **Detects snow cover during twilight (at sun elevations higher than 4º) over land and coast. Except for the additional use of the PseudoR0.6 this test is equal to the Snow Land 3A test.** |

*Table 11: The pure IR components of the grouped threshold tests applied in the cloud screening (these are the only tests being used during night time).*

| Component name (and result) | Used image features | Function |
|---|---|---|
| **Cold Cloud** <br> **(cloud filled) or** <br><br> **(cloud contaminated)** | T11Tsur <br><br> Tsur <br><br> T11T3.7 <br><br> T3.7T12 | **Screens all clouds sufficiently colder than the surface but only if the surface is not too cold.** |
| **Cold Cloud v2014** <br> **(cloud filled) or** | T11T3.7 <br><br> T3.7T12 | **This test measure the departure/deviation of the observed T11t3.7 and T3.7t12 differences from the cloudfree simulations. If they are close to the cloudfree simulations then we have a high** |

| Component name (and result) | Used image features | Function |
|---|---|---|
| (cloud contaminated) | T11Tsur Tsur | **confidence that the FOV is actually cloudfree and therefore require a larger departure in the t11-tsur in order to classify cloudy.** **Instead of applying a definite threshold in the water cloud features T11T3.7 and T3.7T12 as e.g. in the original cold cloud tests (see above) pixels can still be classified cloudy in this test even if the water cloud features have values below such thresholds, provided the cloud top is "cold enough".** |
| **Arctic Warm Cloud** (cloud filled) | T11Tsur T11T3.7 T3.7T12 T3.7_TEXT T3.7T12_TEXT | **Screens all clouds sufficiently warmer than the surface. This test is only applied over sea ice with rather conservative threshold settings. Texture included to avoid classifying ice cracks as clouds.** |
| **Cold Water Cloud** (cloud filled) | T11T3.7 T11Tsur | **Screens sufficiently cold water clouds at night due to their colder appearance in 3.7μm channel.** |
| **Cold Water Cloud Day v2014** (cloud filled) | T11T3.7 T3.7T12 T11Tsur QR0.9R0.6 T11 | **Similar to the Cold Cloud v2014 test described above. But in daytime we also further constrain the test by use of the R0.9/R0.6 quota.** |
| **Water Cloud** (cloud filled) or (cloud contaminated) | T11T3.7 | **Same as above but without temperature restriction.** |
| **Arctic Water Cloud** (cloud filled) | T11T37 T37T12_TEXT | **Aims to detect water or mixed phase clouds over sea ice. The T37T12_TEXT is included to exclude 3.7μm noise that is significant at very cold** |

| Component name (and result) | Used image features | Function |
| --- | --- | --- |
| | | **temperatures.** |
| **Thin Cirrus primary** <br><br> (cloud contaminated) | T3.7T12 | **Screens thin cirrus clouds at night through their warmer appearance at shorter infrared wavelengths (semi-transparency sign).** |
| **Arctic thin Cirrus primary** <br><br> (cloud contaminated) | T37T12 <br><br> T37_TEXT | **Same as above, but we include the T37_TEXT feature over sea ice to avoid misclassifications of leads.** |
| **Arctic thin Water cloud** <br><br> (cloud contaminated) | T37T12 <br><br> T37T12_TEXT | **We use the T37T12 feature with opposite signed thresholds over sea ice to detect transparent clouds that are significant warmer then the underlying surface. The T37T12_TEXT feature is included here to avoid a misclassification of 3.7µm noise.** |
| **Thin Cirrus secondary** <br><br> (cloud contaminated) | T11T12 | **Same as Thin Cirrus Primary Test but using a smaller spectral interval and applied at daytime/twilight.** |
| **Arctic warm Cirrus secondary Test** <br><br> (cloud contaminated) | T11T12 | **Same as above, but with opposite signed thresholds over sea ice to detect transparent clouds that are significant warmer then the underlying surface.** |
| **Arctic thin Cirrus secondary** <br><br> (cloud contaminated) | T11T12 <br><br> T37_TEXT | **We use the T11T12 feature over sea ice with +/- similar threshold settings as the Thin Cirrus Secondary Test to detect cold transparent clouds. To avoid a false detection of leads the T37_TEXT feature is included here.** |
| **Thin Cold Cirrus** <br><br> (cloud contaminated) | T11T12 <br><br> T11Tsur | **Same as above but requiring clouds to be sufficiently cold.** |
| **Highcloud T85T11 land** (cloud contaminated) | T85T11 | **This feature detects high clouds. The idea is that the contrast is better than for the T11T12 case and more robust against sunlight than the T37T12 test.** |

| Component name (and result) | Used image features | Function |
| --- | --- | --- |
| **Highcloud T85T11 sea (cloud contaminated)** | T85T11 | **Same as above but thresholds are calculated for sea surfaces.** |
| **sstNighttime** | T11 T3.7 Tsur T11T12 Satsec:$Cos(\Theta_{sat})$ T11texture | **This test aims at detecting any cloud contaminated pixel over sea, in particular thin cirrus clouds which can have T11 values very close to the predicted surface skin temperature, and may go undetected by the other tests over sea.** **The Sea Surface Temperature (SST) is derived for the pixel using the satellite secant ($Cos(\Theta_{sat})$) and the OSAISAF platform dependent algorithm (see ANNEX A), and the NWP predicted surface skin temperature as the background climatological SST.** **Both the departure between the observed SST and the predicted surface skin temperature (Tsur) and the departure of the observed T11T12 to the predicted cloudfree value is stored.** **The T11T12 departure is the tested against a threshold which depends non-linearly (polynomial in 3$^{rd}$ degree) on the sst-departure. The larger the sst-departure, the larger the T11T12 threshold.** **This means that pixel with a large SST departure needs only a small departure in T11T12 to classify cloudy, but a pixel with a small SST departure requires a large T11T12 departure (a very obvious thin cirrus feature).** **In addition to this the pixel needs to have a slightly raised local texture in T11 compared to the expected cloudfree texture.** |

*Table 12: Components of the grouped threshold tests applied in the cloud screening during day and twilight conditions.*

| Component name<br>(and result) | Used image features | Function |
| --- | --- | --- |
| **Bright Cloud v2014**<br>**(cloud filled)** | R0.6<br><br>T11Tsurf<br><br>QR0.9R0.6<br><br>T11T12<br><br>T11 | **This test aims at capturing low clouds in daytime with top temperatures close to the predicted cloudfree surface temperature and with only a weak cloud signal in the T3.7-T12 feature. These clouds usually have a high reflectance in in the 0.6 band (R06) but as the cloudfree 0.6 reflectance is not adequately simulated for the actual surface relflectance conditions (the simulations are done assuming a static mixture and forrest and open land with no coupling to the actual surface conditions) the threshold offset in this feature has to be set rather high to avoid misclassifying e.g. barren and semi-arid cloudfree areas as cloudy.**<br><br>**The test use the fact that**<br><br>1. **the 11 and 12 micron emissivities of a stratus cloud are nearly equal and that the abundance of water vapour is concentrated beneath and in the cloud deck. Thus the t11 - t12 difference is close to zero and much smaller than the calculated cloudfree threshold.**<br><br>2. **stratus clouds have very high reflectance values in the 0.6 channel**<br><br>3. **daytime stratus clouds seldom have top temperatures above 20 C (measured in the 11 micron channel)**<br><br>4. **clouds have 0.6/0.9 reflectance quotas around and a little below 1.0**<br><br>5. **stratus clouds have daytime top temperatures colder than the cloudfree condition (not warmer!)**<br><br>**Point 3, 4 and 5 above are all safety checks to try to avoid misclassifying cloudfree scenes as cloudy. Of particular concern here are desert or barren land surfaces. Those areas may have dry atmospheres (having low total integrated water content) making the cloudfree t11-t12 low, and may have small scale variations in the 11 and 12 micron emissivity further enhancing a low cloudfree t11-t12. Also desert/barren areas have** |

| Component name (and result) | Used image features | Function |
| --- | --- | --- |
| | | **high cloudfree 0.6 micron reflectivities. But with an upper limit of 293.15K in the t11 many such daytime cases should be avoided. Concerning 1) the information content (or the detection capability) in this feature degrades as the cloudfree atmosphere get's dryer. This means that in general this test will not work as efficient in elevated terrain and at high latitudes. We have made a threshold test dependency trying to account for this, so that it will be harder for a pixel to be classified as cloudy as the t11-t12 threshold gets lower.** |
| **Bright Cloud** (cloud filled) | R0.6 T3.7T12 | **Screens all sufficiently bright clouds, requiring high reflectance in 0.6μm channel and minimum difference in 3.7μm – 12μm channel.** |
| **Bright Cloud Sea** (cloud filled) | R0.6 T11 | **Screens all sufficiently bright clouds, requiring high reflectance in 0.6μm channel and cold cloud tops according to T11.** **This test has marginal effect, if any, since the introduction of more effective daytime tests over sea in v2014. See above. For the same reason the test utilise rather conservative threshold offsets in T11 to avoid misclassifying clear pixels as cloudy.** |
| **Bright Cloud 3A** (cloud filled) | R0.6 QR1.6R0.6 | **Screens all sufficiently bright clouds, requiring high reflectance in both channels, 0.6μm and 1.6μm. The R1.6 threshold is linear in the secant of the satellite zenith angle and is higher in the forward scattering regime.** |
| **Bright Cloud 3A No Sunglint** (cloud filled) | R0.6 QR1.6R0.6 | **Screens all sufficiently bright clouds, requiring high reflectance in both channels, 0.6μm and 1.6μm . Applied outside potential sunglint areas. The R1.6/R0.6 threshold is static and set to 0.32.** |
| **Bright Cloud 3A No Sunglint Land** (cloud filled) | R0.6 QR1.6R0.6 | **Screens all sufficiently bright clouds, requiring high reflectance in both channels, 0.6μm and 1.6μm . Applied outside potential sunglint areas. The R1.6/R0.6 threshold is static and set to 0.32.** |
| **Cold Bright Cloud** (cloud filled) | T11Tsur Tsur | **Same as the cold cloud test but also requires the VIS reflectance to exceed a threshold.** |

| Component name (and result) | Used image features | Function |
|---|---|---|
| | R0.6 | |
| **Cold Bright Cloud 37** (cloud filled) | T11Tsur Tsur R0.6 T3.7T12 | **This test is used under daytime conditions ober land and coast areas. Complementing and to some extent replacing the old "Cold Bright Cloud" test. In addition to the "Cold Bright Cloud" test it also test the T3.7T12 feature.** **The additional use of T3.7-T12 is possible through a more accurate description in v2014 of this feature under cloudfree conditions over land.** |
| **Reflecting Cloud** (cloud filled) | PseudoR0.6 T3.7T12 | **Identifies any reflecting cloud near the night/day terminator. Requires reflection also in 3.7µm channel (separation from snow/ice)** |
| **Reflecting Cloud Sea** (cloud filled) | T11 PseudoR0.6 | **Similar test and purpose as the "Reflecting Cloud" test described above. This test is, however, only applied over sea and coast and doesn't use the T3.7T12 feature.** |
| **Reflecting Cloud 3A (pseudo06CloudTest3A)** (cloud filled) | PseudoR0.6 QR1.6R0.6 | **Identifies any reflecting cloud near the night/day terminator. Requires a R1.6/R0.6 feature higher than 0.45. The threshold in PseudoR0.6 is linear in the sun elevation with the expression: 0.5%Θ + 1.5%, where Θ denotes the sun elevation here).** |
| **Clouds in Sunglint** (cloud contaminated) | R0.6 QR3.7R0.6 T11T12 | **Low (opaque) clouds are separated from cloud free sea in potential sunglint areas when the R3.7/R0.6 ratio is lower than 0.7 and R0.6 exceeds 15%. As an extra precaution the T11T12 difference shall be lower than the threshold for detection of thin cirrus.** |
| **Sunglint 3A** (cloud contaminated) | R0.6 QR1.6R0.6 | **Low (opaque) clouds are separated from cloud free sea in potential sunglint areas when the R1.6/R0.6 ratio is lower than 0.6 and R0.6 exceeds 15%.** |
| **Clouds in Sunglint 3A** (cloud contaminated) | R0.6 QR1.6R0.6 QR0.9R0.6 T11Tsur T11T12 | **This test is applied over coastal regions (no mountains) under both twilight and day conditions, and in open water where sunlint prevails. It relies on the 1.6 micron channel, and the 3.7 micron band is not needed.** **It uses QR1.6R06 to avoid snow and sea ice. It detects mainly low clouds by requiring the T11T12 feature to be lower than the cloudfree** |

| *EUMETSAT Satellite Application Facility to NoWCasting & Very Short Range Forecasting* | Algorithm Theoretical Basis Document for the Cloud Mask of the NWC/PPS | **Code:** NWC/CDOP2/PPS/SMHI/SCI/ATBD/1 **Issue:** 1.0 **Date:** 15 September 2014 **File:** NWC-CDOP2-PPS-SMHI-SCI-ATBD-1_v1_0 **Page:** 34/64 |
|---|---|---|

| Component name (and result) | Used image features | Function |
|---|---|---|
| | | threshold (a low opaque cloud deck will screen the lower part of the atmosphere where the abundance of water vapour is found and which give rise to the main part of the cloudfree T11-T12 difference through a lower transmissivity in at high IR wavelengths and a decreasing temperature with height). The QR0.9R0.6 feature is used to further constrain the test, as cloudy pixels have quota values close to one. |
| **Cold Clouds in Sunglint** (cloud filled) | R0.6 QR3.7R0.6 T11Tsur | Clouds are separated from cloud free sea in potential sunglint areas when the R3.7/R0.6 ratio is lower than 0.7 and R0.6 exceeds 15%. As an extra precaution the cloud shall be sufficiently cold in T11 as compared to the surface temperature. |
| **Cold Clouds in Sunglint 3A** (cloud filled) | R0.6 QR1.6R0.6 T11Tsur | Clouds are separated from cloud free sea in potential sunglint areas when the R1.6/R0.6 ratio is lower than 0.6 and R0.6 exceeds 15%. As an extra precaution the cloud shall be sufficiently cold in T11 as compared to the surface temperature. |
| **Visland Cloud Test** | pseudoR0.6 T3.7T12 | This test is used at twilight and over coastal regions only. It seeks to catch mainly low water clouds or sub-pixel clouds without using the temperature information, but only using the reflective signal in the 0.6 and 3.7 micron bands. |

*Table 13: The components of the grouped threshold tests using texture and spatial information are applied in the cloud screening .*

| Component name (and result) | Used image features | Function |
|---|---|---|
| **Texture Night** (cloud contaminated) | T11_text T3.7T12_text | Pixel with high spatial variations in IR identified as clouds. Difference of infrared channels are used in addition to |

| Component name (and result) | Used image features | Function |
|---|---|---|
| | | **reduce influence from thermal fronts at sea.** |
| **Texture VIS** (cloud contaminated) | R0.6_text | **Pixel with high spatial variations in VIS identified as clouds.** |
| **Texture IR/VIS** (cloud contaminated) | T11_text R0.6_text | **Pixel with high spatial variations in both VIS and IR identified as clouds. High texture in both VIS and IR required in order to avoid mis-classifying thermal fronts.** |
| **Water Cloud Over Water** | T11T3.7-T11T3.7warmest T11-T11warmest Tsur | **The test aim to detect water clouds at night over open sea with cloud tops colder than the sea surface. It tests if the pixel is "more cloudy" in terms of t11 and t37 compared to the warmest (in terms of t11) pixel in a 5 by 5 pixel neighbourhood. To avoid applying the test over sea ice, the NWP predicted surface temperature has to be above a threshold (set to 275 K).** |
| **Bright Cloud Over Water** | Tsur R0.9 T11T11warmest R0.9R0.9warmest | **The test aims at detecting thin and broken clouds over sea at day (including sunglint). It finds the warmest pixel in t11 in a 5 by 5 pixel neighbourhood, and if the following points are fulfilled the pixel is cloud contaminated:**<br><br>• **If the 0.6 micron reflectivity is larger than the for the warmest pixel**<br><br>• **If the 11 micron tb is lower (pixel is colder) than for the warmest pixel minus a static threshold**<br><br>• **If the nwp forecasted/analysed skin temperature is higher than a static offset (this is to avoid testing over potentially sea-ice covered areas)** |
| **SST Daytime Test** | T11 Tsur | **Similar to the SST Nighttime Test. But utilising also the local texture in R0.6 and additional short wave features (R1.6 or** |

| Component name (and result) | Used image features | Function |
|---|---|---|
|  | Satsec:Cos($\Theta_{sat}$)<br>T11T12<br>(R1.6 if available)<br>T11_text<br>QR0.9R0.6<br>R0.6_text<br>(R3.7 if available) | **R3.7 and QR0.9R0.6)**<br>**The daytime OSISAF algorithm is also different and only utilise the T11 and T12 bands, and not the 3.7 micron band which is used in the nighttime algorithm. See ANNEX A.** |
| **SpatialCloudTestLand** | R06, R06warmest<br>T11, T11warmest<br>Tsur | **The test aim at detecting sub-pixel and broken cumulus clouds and thin cirrus clouds over land at day.**<br>**The assumption is that the warmest pixel in a 5x5 neighbourhood is cloudfree or closest to the cloudfree conditions in the features tested, and that if the pixel in question is both significantly colder and brighter, and also have a greater t11t12 difference, then it is most likely contaminated by a cloud.**<br>**The test is bounded by the t11 and predicted surface skin temperature, so that a pixel cannot be cloudy if the t11 is above 34°C or if the Tsur is warmer than 40°C** |

4.1.2.2.2  Threshold tests, per time of the day

*Table 14: The set of grouped threshold tests, used in the different algorithm regimes during day. The grouped tests are listed in the same order as they are applied in the algorithm. The tests are applied in sequence as described in section 4.1.2.8. Pixels will be tested by a variable number of the grouped tests listed, but always in the order shown e.g. in one extreme a coastal pixel may undergo one test*

*(snowLandTest(3A)) during day and the result is a snow/ice contaminated (cloudfree) pixel.. In the other extreme 14 tests may be required for a coastal pixel during day.*

| Environmental regime | Sequence of testing |
|---|---|
| **Day-Coast** | **snowLandTest(3A) snowSeaTest3A_v2014 snowSunglintTest(3A) DriedOutLakesAndRiversTest SaltLakeTest ClearNewWaterBodies brightCloudTest_v2014 coldWatercloudTestDay brightCloudTest(3A) brightCloudTestNoSunglint3Aland coldBrightCloudTest37 thinColdCirrusTest coldCloudsInSunglint cloudsInSunglint(3A) sunglintTest3A coldCloudTestDay_v2014 HighcloudTestt85t11land** |
| **Day-Coast-Mountain** | **snowMountainTest(3A) snowSunglintTest(3A) DriedOutLakesAndRiversTest SaltLakeTest ClearNewWaterBodies brightCloudTest_v2014 coldBrightCloudTest coldWatercloudTestDay brightCloudTest(3A) coldBrightCloudTest37 thinColdCirrusTest coldCloudsInSunglint cloudsInSunglint coldCloudTestDay_v2014 HighcloudTestt85t11land** |
| **Day-Land** | **snowLandTest(3A) snowSunglintTest(3A) ClearNewWaterBodies NotCloudHeavyAerosol brightCloudTest_v2014 brightCloudTest(3A) brightCloudTestNoSunglint3ALand coldBrightCloudTest37 coldWatercloudTestDay(3B only) coldBrightCloudTest thinColdCirrusTest coldCloudTestDay_v2014 HighcloudTestt85t11land SpatialCloudTestLand** |
| **Day-Land-Mountain** | **snowMountainTest(3A) ClearNewWaterBodies NotCloudHeavyAerosol brightCloudTest_v2014 brightCloudTest brightCloudTestNoSunglint3ALand coldBrightCloudTest37 coldBrightCloudTest coldWatercloudTestDay thinColdCirrusTest coldCloudTestDay_v2014 coldCloudTestDay_v2014 HighcloudTestt85t11land** |
| **Day-Sea** | **snowSeaTest(only 3B) snowSeaTest3A_v2014 DriedOutLakesAndRiversTest SaltLakeTest coldBrightCloudTest brightCloudTest(3A) coldWatercloudTestDay brightCloudTestNoSunglint3A thinCirrusSecondaryTest textureIrvisTest textureVisTest textureNightTest brightCloudTestSea brightCloudOverWaterTest sstDaytimeTest HighcloudTestt85t11sea** |
| **Day-Sea Ice** | **snowSeaTest(3A) coldCloudTest coldBrightCloudTest brightCloudTest(only 3B) coldWatercloudTest brightCloudTestNoSunglint3A coldCloudTest thinCirrusSecondaryTest brightCloudTestSea coldCloudTest_v2014 HighcloudTestt85t11sea** |
| **Day-Sunglint** | **snowSunglintTest(3A) DriedOutLakesAndRiversTest SaltLakeTest** |

| Environmental regime | Sequence of testing |
|---|---|
| | **thinCirrusSecondaryTest textureIrvisTest coldBrightCloudTest coldCloudsInSunglint(3A) brightCloudTest(only 3B) cloudsInSunglint(3A) coldCloudTest brightCloudTestSea brightCloudOverWaterTest HighcloudTestt85t11sea** |

*Table 15: The set of grouped threshold tests, used in the different algorithm regimes during night. The grouped tests are listed in the same order as they are applied in the algorithm. The tests are applied in sequence as described in section 4.1.2.8.*

| Environmental regime | Sequence of testing |
|---|---|
| **Night-Coast** | **coldClearArcticAreaTest coldCloudTest coldWatercloudTest watercloudTest  thinCirrusPrimaryTest thinCirrusSecondaryTest coldCloudTest_v2014  HighcloudTestt85t11land** |
| **Night-Coast-Inversion** | **coldClearArcticAreaTest watercloudTest coldWatercloudTest coldCloudTest  thinCirrusPrimaryTest thinCirrusSecondaryTest coldCloudTest coldCloudTest_v2014 HighcloudTestt85t11land** |
| **Night-Coast-Mountain** | **(Identical to the Night-Land-Mountain scheme.)** |
| **Night-Land** | **coldClearArcticAreaTest coldCloudTest coldWatercloudTest watercloudTest (only outside desert) thinCirrusSecondaryTest thinCirrusPrimaryTest coldCloudTest_v2014 HighcloudTestt85t11land** |
| **Night-Land-Inversion** | **coldClearArcticAreaTest waterCloudTest coldWatercloudTest thinCirrusSecondaryTest thinCirrusPrimaryTest coldCloudTest coldCloudTest_v2014 HighcloudTestt85t11land** |
| **Night-Land-Mountain** | **coldClearArcticAreaTest  waterCloudTest (only outide desert) coldWatercloudTest coldCloudTest thinCirrusPrimaryTest thinCirrusSecondaryTest coldCloudTest_v2014 HighcloudTestt85t11land** |
| **Night-Sea** | **waterCloudTest thinCirrusPrimaryTest textureNightTest coldCloudTest coldWatercloudTest watercloudOverWaterTest coldCloudTest coldCloudTest_v2014 HighcloudTestt85t11sea** |
| **Night-Sea Ice** | **ArcticwaterCloudTest coldCloudTest ArcticthinCirrusPrimaryTest ArcticthinwaterCloudTest ArcticwarmCloudTest ArcticwarmCirrusSecondaryTest ArcticthinCirrusSecondaryTest HighcloudTestt85t11sea** |

*Table 16: The set of grouped threshold tests, used in the different algorithm regimes during twilight. The grouped tests are listed in the same order as they are applied in the algorithm. The tests are applied in sequence as described in section 4.1.2.8.*

| Environmental regime | Sequence of testing |
|---|---|
| **Twilight-Coast** | **snowLandTest(3A) snowSunglintTest(3A) snowTwilightTest(3A) coldClearArcticAreaTest coldCloudTest reflectingCloudTest(pseudo06CloudTest3A) thinColdCirrusTest reflectingCloudTestSea coldWatercloudTest watercloudTest vislandCloudTest coldCloudTest thinCirrusSecondaryTest thinCirrusPrimaryTest cloudsInSunglint(3A) sunglintTest3A coldCloudTest_v2014 HighcloudTestt85t11land** |
| **Twilight-Coast-Inversion** | **snowLandTest(3A) snowSunglintTest(3A) snowTwilightTest(3A) coldClearArcticAreaTest reflectingCloudTest(pseudo06CloudTest3A) thinColdCirrusTest coldCloudTest watercloudTest vislandCloudTest thinCirrusSecondaryTest thinCirrusPrimaryTest cloudsInSunglint(3A) coldCloudTest_v2014 HighcloudTestt85t11land** |
| **Twilight-Coast-Mountain** | **(Identical to the Twilight-Land-Mountain scheme.)** |
| **Twilight-Land** | **snowLandTest(3A) snowSunglintTest(3A) snowTwilightTest(3A) coldCloudTest reflectingCloudTest(pseudo06CloudTest3A) coldWatercloudTest watercloudTest thinCirrusSecondaryTest thinCirrusPrimaryTest coldCloudTest_v2014 HighcloudTestt85t11land** |
| **Twilight-Land-Inversion** | **snowLandTest(3A) snowTwilightTest(3A) coldClearArcticAreaTest rflectingCloudTest (pseudo06CloudTest3A) thinColdCirrusTest watercloudTest thinCirrusSecondaryTest thinCirrusPrimaryTest coldCloudTest coldCloudTest_v2014HighcloudTestt85t11land** |
| **Twilight-Land-Mountain** | **snowMountainTest(3A) snowTwilightTest(3A) coldClearArcticAreaTest  brightCloudTest3A coldBrightCloudTest coldWatercloudTest coldCloudTest coldCloudTest_v2014 coldCloudTest  watercloudTest thinCirrusSecondaryTest thinCirrusPrimaryTest HighcloudTestt85t11land** |
| **Twilight-Sea** | **snowSeaTest(3A) thinCirrusSecondaryTest textureIrvisTest textureNightTest   coldCloudTest reflectingCloudTest(pseudo06CloudTest3A) coldWatercloudTest watercloudTest coldCloudTest reflectingCloudTestSea coldCloudTest_v2014 HighcloudTestt85t11sea** |
| **Twilight-Sea Ice** | **snowSeaTest(3A) thinCirrusSecondaryTest textureIrvisTest coldCloudTest reflectingCloudTest(pseudo06CloudTest3A) coldWatercloudTest watercloudTest coldCloudTest** |

| Environmental regime | Sequence of testing |
|---|---|
| | **coldCloudTest_v2014 HighcloudTestt85t11land arcticthinCirrusPrimaryTest** |
| **Twilight-Sunglint** | **coldCloudTest coldBrightCloudTest coldCloudTest thinCirrusSecondaryTest textureIrvisTest HighcloudTestt85t11sea** |

### 4.1.2.3 Low level temperature inversions

Separation of low clouds and cloud free land or water surfaces during night and in twilight sometimes becomes a particular challenging, if not impossible, task using satellite data alone.

In the absence of sunlight the brightness temperature difference between the 11 and 3.7µm channels is normally large enough to allow detection of low water clouds. However, exceptions do occur where this difference is so small that separation from the cloudfree case becomes ambiguous. Over the open ocean low clouds may contain rather large water droplets and during the mid to high latitude winter season low clouds may sometimes consist of a sufficiently high amount of ice particles. In both cases the shortwave IR emissivity at the cloud top is high enough so as to erase the normally existing 11 minus 3.7µm brightness temperature difference.

When the sun is just above the horizon the 3.7µm brightness temperature is raised due to the additional radiance from reflected sunlight, and water cloud detection using the 11 and 3.7µm brightness temperature difference is impossible. The configuration employed the AVHRR/3 on some of the polar orbiters (see section 4.2.2.1.1) where the channel 3A and channel 3B are switched passing between day and night does not eliminate this problem. First as the switching is done from one line to another there will inevitably be regions without sunlight and without channel 3B data. Secondly even with the sun above the horizon the 1.6µm reflectance signal might not be sufficiently strong in order to be used unambiguously to separate water clouds from cloud free land surfaces.

In the above described situations the only possibly useful feature is the difference in the surface temperature and the 11µm brightness temperature. However, it requires that the cloud top is sufficiently colder than the surface, and this is not always the case. Especially over land and during the winter season low level temperature inversions are normally quite frequent, and the cloud top is often as warm as or even warmer than the surface (the latter phenomena is often referred to as black stratus in satellite remote sensing).

Comparing radiosonde and Hirlam profiles, we found using the temperature difference between 950hPa and the surface that Hirlam is generally capable of correctly detecting the presence of low level inversions in wintertime situations over northern Europe, even though the strength is often not correct. The 950hPa level may seem rather low, but the situations we are after are those occurring in stationary situations with usually a rather high surface pressure. No attempt is made to detect inversions in high terrain and over sea ice, as NWP profiles are less reliable in lower levels here. For the same reason the threshold offset in T11 is generally set rather high in mountainous terrain and over sea ice.

The presence of a low level inversion as detected with this method is a direct indication of high risk for significant errors in the estimated surface temperature (frequently the skin temperature is much lower in reality). If an algorithm were to ignore such expected errors and rely on the T11 only and its threshold (derived assuming a correct skin temperature) cloudfree areas at night or in twilight would frequently be misclassified as cloudy.

When a low level inversion is detected a particular bit in the processing flags dataset is set implicitly indicating low quality (see sections 4.2.1 and 4.2.3). If the inversion is strong defined by $T_{surface}$ - $T_{950hPa} \leq$ 5K no cloud detection using only the T11 feature is attempted, and thus certain wintertime stratus and areas of water clouds in twilight may remain undetected. But if the inversion is weak or non-present according to the NWP model, the T11 feature is utilised to detect cold low clouds without any clear nighttime water cloud signal in the T11 - T37 feature.

In case of a weak inversion the observed brightness temperature at 11µm has to be 17K lower than the cloudfree simulation using the forecasted, and often erroneously too warm, surface temperature, whereas in areas of no risk of low level inversions the corresponding offset is 8K (12K in mountainous terrain).

### 4.1.2.4  Probability for sunglint

The probability for sunglint is calculated using the formula derived by Berendes et al. (1999) which depends purely on the sun-satellite viewing geometry. Berendes et al. derived their formula from the distribution found by Cox and Munk (1954) assuming an isotropic average wind field with wind speeds in the range of 0 to 14m/s. We use this probability of sunglint measure only as an indicator of risk for sunglint. If the probability is larger than a threshold, currently set to 1.0%, we activate the processing flag for presence of sunglint and invoke specially designed sunglint threshold sequences.

### 4.1.2.5  Desert and barren areas

The PPS cloud algorithms were foremost developed for applications at high and mid latitudes, such as encountered in central and northern Europe and adjacent seas. However, the PPS cloudmask has been tested and improved for the purpose of cloudmasking over the whole world. The surface conditions, concerning the spectral emissivities and reflectivities over desert and semi arid areas are considerably different from the surfaces (mixed open land and forest) for which the PPS was developed and tuned. This is most pronounced for the 3.7µm channel whose emissivity is substancial less than 1. Additionally, the short wave reflectivities are high over desert sands. Therefore these extreme conditions have been tackled by a special treatment in earlier versions..

In version 2014 we introduced a surface treatment which includes the solar contributions especially for the 3.7µm channel. With the explicit use of surface emissivity and reflectivity any special procedure for certain land classes becomes redundant or even deteriorating. Therefore, the USGS land cover characterization is used only to distinguish between land and sea pixels.

## 4.1.2.6  Definition of mountainous terrain

Mountainous terrain pose problems for the PPS cloud mask for several reasons, the most important ones are listed here below:

1. Sloping terrain within the AVHRR/VIIRS FOV resulting in locally changing sun-satellite viewing conditions and shadows, altering the surface reflectance.

2. Locally varying terrain height on a scale not resolved by the NWP model topography. This may result in an actual average elevation over the AVHRR/VIIRS FOV which is far from the elevation given by the model topography, and consequently the NWP parameters, and in particular the forecasted/analysed surface skin temperature, may deviate substantially from the truth.

3. A highly varying topography (on the scale of a few hundred meters to a few kilometers) enhance small scale climate variability usually not well captured by an NWP model with a resolution of several km (say 10 or more). This is related to point 2 above.

4. Highly elevated terrain (including plateus, not necessarily with a high local variation in topography) in general give rise to colder temperatures. Very cold surface conditions reduce the signal to noise especially in the longwave IR region around 3.7 microns, which is a crucial spectral band for nighttime cloud detection.

As shadows are not explicitly handled in the algorithm, and since surface reflectance is modelled after a completely flat earth surface over the FOV, the issue raised in point 1 degrades the daytime cloud detection features based on the short wave spectral bands (0.6, 0.8, 1.6 and 3.7 microns). Under point 1 conditions the algorithm needs to be careful not to go as close to cloudfree

thresholds as it is possible over more gentle terrain. Point 2 and 3 requires the cloud mask algorithm to be more cautious especially in the use of the surface skin temperature in terrain with high local variability in elevation, as it is more prone to be wrong here.

Point 4 is actually implicitly treated by the NWP model as long as the terrain is only varying slowly in elevation over horizontal scale comparable to the NWP grid resolution. If the terrain is highly variable, the problem is already described by point 2 and 3.

Due to these potential problems PPS is using a static map that distinguish gentle terrain, with variations in elevation which are small over a scale comparable to the NWP grid resolution, from rough terrain with variations in elevation which are large over the NWP grid cell. Before PPS-v2014 the distinction between gentle and rough terrain was done purely on the 1km resolution digital elevation map (USGS GTOPO 30, see further on). From version 2014 we derive a roughness map from the 1km elevation data, by deriving the standard deviation of the elevation in meters over a local 11 by 11 pixel kernel. The threshold delineating gentle from rough terrain is set to 1000m. In version 2012 end earlier the threshold was 500m on elevation.

There is a rather good correlation between roughness (as defined above) and elevation over the European area and thus the general impact of this change is modest on average over Europe. However, on a global scale there are substantial differences between the two means of identifying rough terrain as can be seen from Figure 1, Figure 2, and Figure 3. Especially over the East Asian areas and over large parts of Africa and Antarctica the differences are significant.
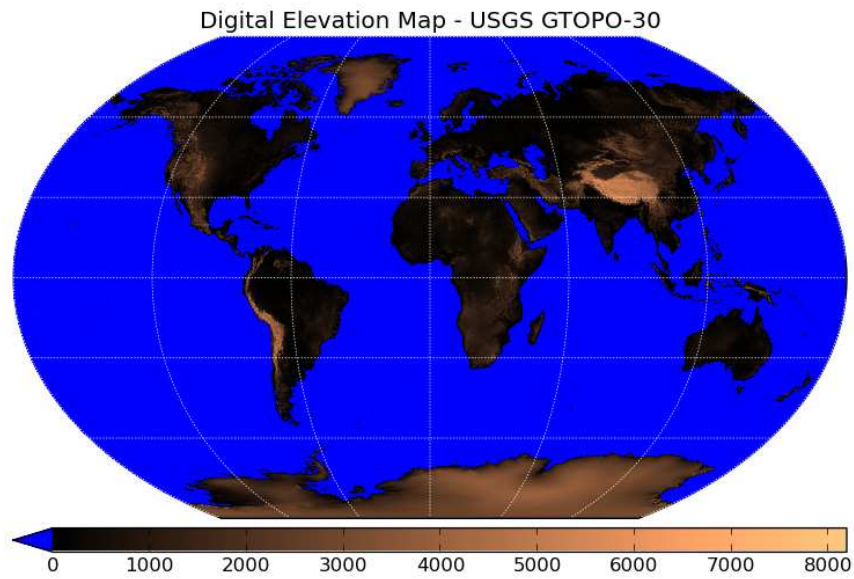
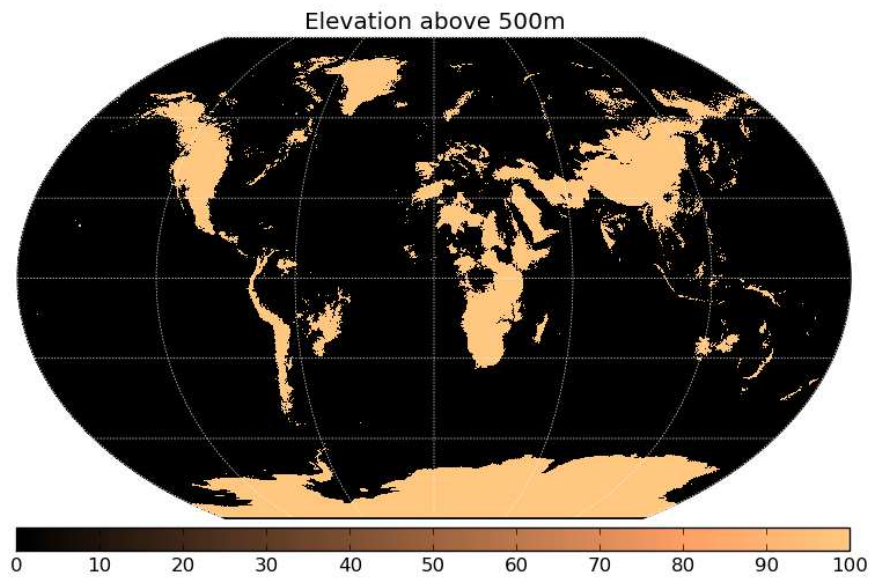*Figure 1: The digital elevation map used in PPS*



*Figure 2: Global map highlighting areas on the earth with an elevation above 500 meters. The 500 meter limit was used previously in PPS to delineate low-land from mountainous terrain.*

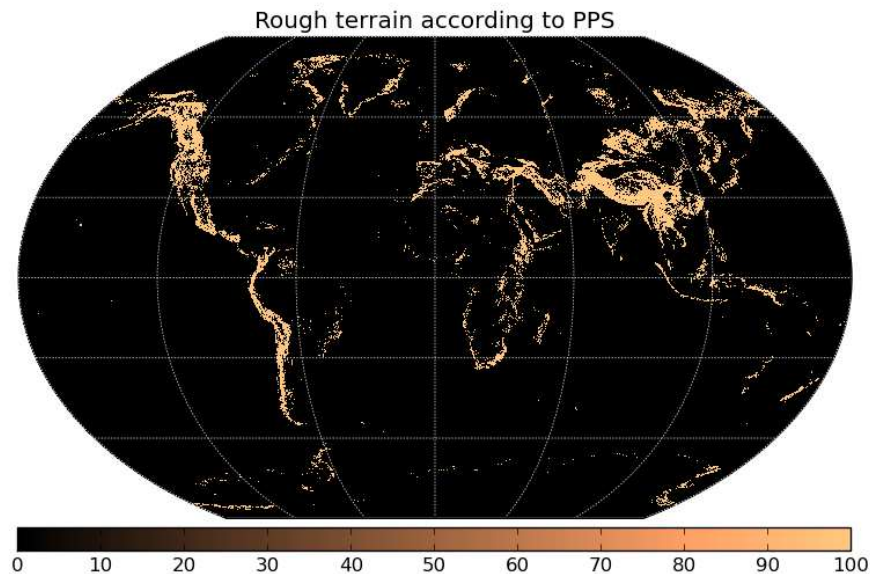| EUMETSAT Satellite Application Facility to NoWCasting & Very Short Range Forecasting | Algorithm Theoretical Basis Document for the Cloud Mask of the NWC/PPS | **Code:** NWC/CDOP2/PPS/SMHI/SCI/ATBD/1<br>**Issue:** 1.0 **Date:** 15 September 2014<br>**File:** NWC-CDOP2-PPS-SMHI-SCI-ATBD-1_v1_0<br>**Page:** 44/64 |
|---|---|---|

*Figure 3  Global map showing where on earth the terrain is rough according to PPS. This is the dataset used in PPS from version 2014 to deliniate rough/mountanous terrain from low-land/gentle terrain.*

### 4.1.2.7  Definition of sea ice surface

We have adapted the PPS software for cloud product generation over sea ice. The cloud detection is very problematic over sea ice during night-time because of 1) the unreliability of the NWP surface temperature prediction over ice, 2) the frequent occurrence of temperature inversion, i.e. clouds have often similar temperatures as the ice surface and, 3) the extreme low temperatures leading to a very high noise to signal ratio in the 3.7µm channel (most pronounced for the AVHRR instrument). During daytime misclassifications of thin fog layers, occurring frequently over sea ice during spring and fall, were observed and the software was adapted accordingly.

The surface conditions over sea ice are rather different then surface conditions over open ocean or land surfaces and we have thus decided to use the OSISAF sea ice product to define a different environmental regime. We define the open ocean as 'ice covered' if the sea ice concentration is higher then 30 % or in case an ice map is not available, if the NWP ice surface temperature definition is significant below 273 K over open ocean. The OSISAF product does not contain data around the pole, but we consider this area as being constantly ice covered.

### 4.1.2.8  Accounting for a changing land cover with time

Due to the ongoing global climate change and increasing man-made impact (e.g. dams for water power or heavy and sustained irrigation) on the earths resources, or simply because of natural

seasonal variations, it happens that the USGS land use dataset show water in some locations where it actually is land at the time of the satellite data retrieval. Or vice versa, the land use dataset might show land where there actually is water. Figure 4 illustrate a case where the land use shows a lake of a certain size, while one can see in the satellite image that the actual size of the lake is significantly smaller.

To cover up for some of such situations we have introduced a number of clear tests (*Clear New Water Bodies*, *Salt Lake Test* and *Dried Out Lakes And Rivers Test*) as outlined in Table 8.
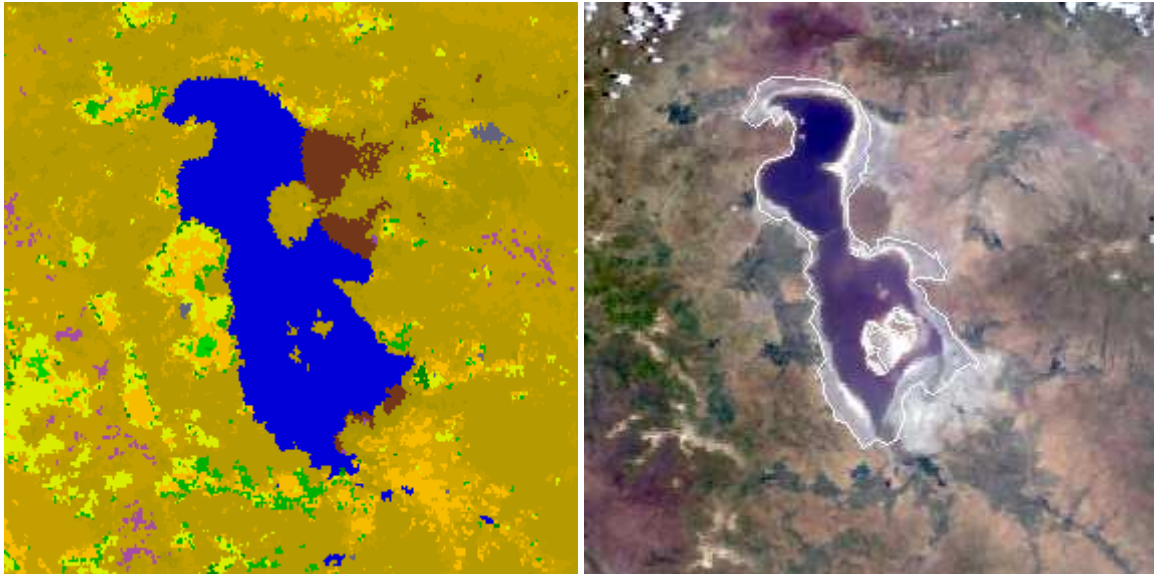


*Figure 4: Usgs Landuse map (left) and S-NPP VIIRS True Color image taken June 5th, 2013, 10:41 UTC received and processed at SMHI. The area in focus is the Lake Urmia in Northeastern Iran.*

### 4.1.2.9 Other clear screening test

In version 2014 CMa several clear screening tests have been included. These are performed before the cloud tests. A part from the test accounting for changing land cover there are one test that checks for very cold (below 230K) clear areas during night. In these conditions the temperatures are so low that cannel 3.7 often have nodata and can not be used for any tests. The other new clear test screens for very heavy aerosols to not misclassify these as clouds. See Table 8 for all clear tests and descriptions.

### 4.1.2.10 Test sequence

The algorithm consists of a sequence of grouped threshold tests. In a grouped threshold test, several of the features listed in Table 7 are tested together. In order for a grouped threshold test to be successful (decisive), all feature tests constituting the particular grouped test have to be successful for the given pixel.

As the dynamic thresholds have been derived from RTM simulations of cloud free land and ocean surfaces in absence of snow cover (or sea ice), an identification and screening of snow covered cloud free surface are attempted prior to any cloud or clear screening tests. All clear screening tests are

done before the cloud screening tests. The set of grouped threshold tests used in the snow screening clear screening, and in the cloud screening are listed in Table 8, Table 9, Table 10, Table 11, Table 12, and Table 13.

Some degree of fuzziness is introduced in the thresholding, by keeping track of the feature distances to the thresholds. The test sequence is continued until a grouped threshold test is successful and all of its feature tests are passed with a safe margin. That is, all features in the grouped test are sufficiently far away from the thresholds if the test is to be decisive.

First of all pixel is set to 1 (*clear*). If the test is passed and all of the features have values far away from their corresponding thresholds the output is set to *1 (clear, only for clear tests)* 2 (*snow/ice contaminated*), 3 (*cloud contaminated*), or 4 (*cloud filled*) depending on the purpose of the test, and the test sequence is stopped; the low quality flag is unset if set. If the test is passed but one or more of the features have values close to their corresponding threshold the output is set to 2, 3, or 4 depending on the purpose of the test, a dedicated *low quality flag* is set, and the test sequence is continued. The thresholding algorithm is logically divided in a number of sub-algorithms depending on the actual situation in terms of

- Illumination: day/twilight/night

- Geography: land/coast/sea/sea ice

- Topography: Mountaneous terrain with high local scale roughness or gentle/smooth terrain (plateau or low land)

- Sunglint

- Presence of low level temperature inversion


All the above variables put special requirements on the algorithm. Different environments and illumination conditions require different feature tests and sometimes also different thresholds or threshold offsets.

Sunglint is the specular reflection of sunlight over water surfaces, and is thus only considered over *coast* and open *sea surfaces*. Furthermore we only consider low level temperature inversions during night and twilight over land and coast, and only in low terrain. The presence or not of temperature inversions are relevant only when testing the observed $T11$ ($T11$) against the forecasted surface temperature. During day other more effective features are always available and furthermore temperature inversions are far less frequent. See section 4.1.2.2.2 for the motivation of the inclusion of the inversion variable.

Potentially this gives eight different *land* algorithms, thirteen different *coast* algorithms, and eight different *sea* algorithms. Thus in total 24 different algorithms. However, in our implementation we distinguish only between eight *coast* algorithms instead of thirteen, as we implicitly treat the sunglint problem within the three twilight and the two day algorithms. The 24 different algorithms and the sequence of the applied grouped threshold tests are listed in , Table 15, and Table 16.

Observe that it is possible to have high terrain in a coastal area, as is the case e.g. along large parts of the Norwegian coast (at many places fjords cut into rather rough terrain where the topography within the instruments FOV may vary as much as from sea level to around 2000 meters above sea level). Furthermore since the FOV may be over both water and low land at the same time one may encounter problems of both sunglint and the presence of low level inversions.

## 4.2 PRACTICAL CONSIDERATION

### 4.2.1 Quality control and validation

*Table 17: Offsets (safety margins) for quality assessment applied to the CMa thresholding.*

| Cloud test | R0.6 | PseudoR0.6 | R1.6 | R3.7 | QR1.6R0.6 | QR0.9R0.6 |
|---|---|---|---|---|---|---|
| **Offset margin** | 2.0% | 0.5% | 2.0% | 1.0% | 0.06 | 0.10 |
| **Cloud test** | QR3.7R0.6 | T11 | T11T3.7 | T11T12 | T3.7T12 | T11Tsur |
| **Offset margin** | 0.06 | 1.0K | 0.30K | 0.30K | 0.30K | 1.0K |
| **Cloud test** | R0.6_text | T11_text | T3.7T12_text | | | |
| **Offset margin** | 0.15 | 0.15 | 0.15 | | | |

Some offsets differ between GAC settings and non-GAC settings, but the values in Table 17 are valid for both cases.

As outlined in detail in section 4.2.3 a set of processing flags are included in the CMa product. One of these flags may be used directly as a quality indicator of the pixel classification. The procedure on how this *low quality* flag is being set has been outlined in section 4.1.2.10:

- a pixel classified as cloudy is flagged *low quality* (cloud mask result is associated with low confidence) if no cloud detection test was really successful. A threshold test is considered really successful only if the difference between the threshold and the measurement is larger than a test dependent offset or safety margin. Table 17 lists the offsets applied.

- a pixel classified as cloud free is flagged *low quality* if the difference between a feature threshold and its observed (measured) value is lower than the offset associated with that feature (see Table 17) for at least one grouped cloud test.

- a pixel classified as snow/ice contaminated is flagged *low quality* if the difference between a feature threshold and its observed (measured) value is lower than the offset associated with that feature (Table 17) for the grouped snow/ice detection test or at least one grouped cloud test.

*Table 18 Accuracy measures and verification scores for the CMa (version 2014) for 99 orbits of AVHRR-GAC data 2006-2009 compared to CALIPSO.*

| Observed Accuracy --- AVHRR GAC Global data | | | | | | |
|---|---|---|---|---|---|---|
| | Hitrate | POD-cloudy% | FAR-cloudy % | POD-clear % | FAR-clear % | N |
| PPS GAC (all) CLARA-A1 v2010 | 0.76 | 73.4 | 8.4 | 82.3 | 45.9 | 725900 |
| PPS GAC (all) v2014 | 0.77 | 75.0 | 9.9 | 82.3 | 39.7 | 7850434 |

*Table 19: Accuracy measures and verification scores for the CMa (version before 2005) as compared to the Synop reports, for all winter cases and those with and without the presence of low level temperature inversion. ma is the mean absolute error in octas. h is the hit rate where cloudy is defined as 6 to 8 octas and cloud free as 0 to 2 octas, and all cases with a Synop cloud cover between 3 and 5 (both inclusive) are not considered. Pod stands for probability of detection, and far is the false alarm rate. N is the total number of Synop-satellite comparisons.*

| | Ma | H | bias[%] | Pod$_{cloud}$ | far$_{cloud}$ | pod$_{clear}$ | far$_{clear}$ | N |
|---|---|---|---|---|---|---|---|---|
| **Winter** | 1.59 | 0.884 | 1.9 | 0.938 | 0.062 | 0.659 | 0.341 | 55947 |
| **Winter No Inv** | 1.38 | 0.909 | 4.2 | 0.966 | 0.034 | 0.589 | 0.411 | 36592 |
| **Winter Inv** | 2.00 | 0.830 | -2.4 | 0.856 | 0.134 | 0.741 | 0.260 | 10355 |

In addition to the *low quality* flag there are further processing flags which indirectly provide information on the reliability or quality of the CMa output. For instance, it is well known that cloud detection is more difficult during night and twilight as compared to day, and this is also reflected in the cloudmask validation results (see validation report of pps v2014, Dybbroe et al. (2005b)). Likewise, the presence of low level temperature inversions over land and sunglint over sea, should raise a warning indicating lower reliability. The CMa processing flags include a flag for high risk of sunglint and a flag for presence of low level inversions, which may be used to sort out these pixels.

Despite a much improved cloud detection in sunglint as compared to SCANDIA for instance as reported in Dybbroe et al. (2005b) it still happens quite frequently that the CMa mistakes cloud free sea in sunglint for clouds. Table 19 summarise the validation results for winter cases with and without low level inversions for PGE01 version before 2005. More details on the Synop satellite comparison can be found in Dybbroe et al. (2005b). Results for PGE01 v2014 compared with CALIPSO data show that POD-cloudy is lower (-15%) when there are inversions present. However, POD-clear is better (2.5%) for inversion conditions. This indicates that cloudy pixels during inversion conditions are not expected to be of lower quality. (Data compared was 150 thousands

| *EUMETSAT Satellite Application Facility to NoWCasting & Very Short Range Forecasting* | Algorithm Theoretical Basis Document for the Cloud Mask of the NWC/PPS | **Code:** NWC/CDOP2/PPS/SMHI/SCI/ATBD/1 |
|---|---|---|
| | | **Issue:** 1.0      **Date:** 15 September 2014 |
| | | **File:** NWC-CDOP2-PPS-SMHI-SCI-ATBD-1_v1_0 |
| | | **Page:** 49/64 |

matched locally received avhrr/viirs pixels over land during night/twilight and inversion/not inversion conditions).

Comparison between CMa v2012 and v2014 show that POD-clear and POD-cloudy is improved and that there are less nodata pixels in the cloudmask (higher N). See the validation report of PPS v2014 and Table 18 for more detailed results.

The CM SAF cloud dataset CLARA-A1, used PPS version 2010 to retrieve cloud mask. CLARA-A1 has been validated against CLOUDSAT/CALIPSO (see Karlsson and Johansson 2013 and Karlsson et al. 2013). For the Metop validation against CLOUDAT/CALIPSO it is unfortunately only possible for arctic regions due to overlap constrains of orbits. See also Karlsson and Dybbroe, 2010 for validation of earlier version of PPS in the Arctic.

## 4.2.2  List of inputs

### 4.2.2.1  Satellite data

The algorithm has been developed specifically for the Advanced Very High Resolution Radiometer (AVHRR) on board the current and future polar orbiting NOAA and EUMETSAT Metop satellites. It has been implemented so that it automatically handles both AVHRR/2 data, with channel 3B during both day and night, and AVHRR/3 data, with channel 3B during night and 3A during day.

Table 3 lists the set of channels of the AVHRR/3. All channels are mandatory for the CMa. Efforts have been made to widen the applicability of the PPS to other instruments on polar platforms. Up to now it is possible to process MODIS data, data from VIIRS on the Suomi-NPP and preparations have been done (as far as possible) for future JPSS satellites. See Table 20 for a complete set of channels.

*Table 20: The channels, which are used for the cloudmask classification.  Mandatory and optional channels are specified. Either the 1.6µm channel or the 3.7µm channel has to be available. The 3.7µm channel is, however, mandatory for the aerosol flag output (see section 4.2.3).*

| λ(µm) | 0.6 | 0.9 | 1.6 | 3.7 | 8.5 | 11 | 12 |
| --- | --- | --- | --- | --- | --- | --- | --- |
| | **mandatory** | **mandatory** | **At least one of them is mandatory** | | **optional** | **mandatory** | **mandatory** |

The instrument data being input to the CMa are calibrated, geo-located (navigated) and mapped to the specific geographical projection and area of interest or processed on the whole satellite swath. For AVHRR, the calibration, geo-location and remapping is done outside the CMa by the PPS common functions (AHAMAP) taking either AVHRR level 1b (AAPP definition) data as generated by AAPP, or archived level 1b NOAA LAC data. The latter is not a SAF requirement.

#### 4.2.2.1.1  AVHRR channel 3A/3b commutation scheme

The AVHRR/3 instrument has 6 spectral channels available. However, due to a fundamental constraint in the AVHRR only data from five channels can be transmitted to ground at the same time. As a consequence a switching or selection of the channel 3A (1.6µm) and 3B (3.7µm) data stream has to be made. The commutation scheme currently in effect is so that all current NOAA satellites except NOAA-17, transmit only data from channel 3B. Only on NOAA-17 an automatic switching is performed so that in daytime channel 3A is provided and during night-time the channel 3B is the active. The switching is performed when the satellite passes a day-night terminator.

***NB!*** It is worth mentioning that the switching will sometimes result in situations with only two useful channels (the IR channels 4 (11µm) and 5(12µm)) available, in contrast to three (channels 3B, 4, and 5) when no switching is performed. This is when channel 3A is active and part of the scan the sun is below the horizon.

For the VIIRS instrument channel M10 and M12 (respectively channel I3 and I4 in the higher spatial resolution), corresponding to the AVHRR channels 3A and 3B, are usually both available at the same time.

### 4.2.2.2  Sun and satellite angles

The instantaneous sun-satellite viewing geometry is stored for every satellite FOV. The angles are the sun zenith angle ($\theta_{sun}$), the satellite zenith angle ($\theta_{sat}$) and the sun-satellite azimuth difference angle as well as the sun and satellite azimuth angles. The satellite zenith angle is always positive and increases from 0° at the sub-satellite point to about 68° at the edges of the swath. The azimuth difference is defined as

$$\delta\phi = \begin{cases} 360° - \delta\phi' : \delta\phi' > 180° \\ \delta\phi' \qquad : \delta\phi' \leq 180° \end{cases}$$

Where $\delta\Phi' = |\Phi_{sun} - \Phi_{sat}|$. Here $\Phi_{sun}$ is the sun azimuth (counted clockwise from the local north) and $\Phi_{sat}$ is the satellite azimuth. Surface specular reflection on a perfect mirror will be observed by the satellite when $\delta\Phi = 180°$ provided the sun zenith angle equals the satellite zenith angle.

The sun zenith angle is used to define what we refer to as day, night and twilight, used when structuring the algorithm in different test sequences using different grouped threshold tests and different threshold offsets. According to the definition used here it is day when $\theta_{sun} \leq 80°$, night when $\theta_{sun} \geq 95°$, and twilight for values of $\theta_{sun}$ in between.

The sun-satellite angles are mandatory for the CMa. They are derived from the AAPP level 1b file (or the corresponding NOAA LAC data) by using (rather extensive and expensive) interpolation and extrapolation (see [RD.2.]).

### 4.2.2.3  Land cover characterisation and elevation

We use the 1km global land cover characterisation database available from the Unites States Geological Survey (USGS) (see Anderson et al., 1976 and Eidenshink and Faundeen, 1994), mainly for separating land and water surfaces, but also to identify barren and desert areas where shortwave IR emissivities are significantly below 1 (Salisbury and d'Aria, 1994). Digital elevation model (DEM) data is derived from the *Global 30 arc seconds topography database*, GTOPO30, (http://edcdaac.usgs.gov/gtopo30/) and used to separate low and gentle terrain from high and rough mountaneous terrain.

The native elevation and land-use data are being processed and mapped onto the swath of each scene by the PPS software to produce land-use, elevation, roughness, and fraction of land maps. See [RD.2.] for a description of how to generate physiography data for a scene. The physiography data are mandatory for the CMa.

## 4.2.2.4 Surface Infrared emissivity data

For calculating the threshold tables varying land surface infrared emissivity data has been taken into account. The global land surface emissivity data used is the standard MODIS product, MYD11C3 (Version 005)..

In the PPS software package is included a number of emissivity files, which contains a climatology of the described emissivity data from ten years of data (2003-2012), and mapped to tiles.

## 4.2.2.5 Sea ice data

Sea ice data can be provided optional to the PPS cloud masking algorithm to define the presence of sea ice. We use the ice concentration map from the OSISAF to define the environmental regime 'sea ice'. The sea ice schemes are used in case the ice concentration is higher then 70 %. If no ice data are provided, the NWP surface temperature is checked over open ocean. If this temperature is significant below 273 K , the sea ice cloud masking schemes are switched on.

Either operational or re-processed ice concentration map from OSISAF can be used.

## 4.2.2.6 NWP data

The CMa algorithm needs a reliable estimate of the column integrated water vapour content, the surface (skin) temperature, and the temperature at the 950 hPa level, in full (map-projected) pixel resolution. The total water vapour column and surface temperature are input to the derivation of the dynamic thresholds, and the temperatures at the surface and 950 hPa are used to identify low level temperature inversions.

These data are extracted from NWP model output. For Nowcasting purposes time is critical and therefore the PPS system will attempt to derive the thresholds and mapped NWP parameters prior to the satellite overpass. The system is configured by default to look for both analysis fields and short range forecasts with lead times between 6 and 24 hours from the configured NWP model. The lower limit of 6 hours is in order to avoid possible problems related to model spin-up. When possible (eg. for re-processing) PPS can be configured to use a valid (close in time to the satellite overpass) NWP analysis.

The PPS will extract raw NWP data in Grib format and generate the required parameters to the swath. There is, however, a minimum requirement for the content of the NWP Grib file in order for PPS to generate the parameters mentioned above. See [RD.2.] for these minimum requirements.

## 4.2.2.7 Parameter files and algorithm configuration files

The CMa only has a few configuration parameters related to how much is wanted in the final output. These can be found in the file pps_config_common.cfg and are listed here:

- GENERATE_CLOUDMASK (default yes): Whether the cloud mask main output is wanted.

- GENERATE_PROCESSING_FLAG (default yes): Whether the processing flags are wanted.

- GENERATE_TEST_FLAG (default yes): Whether the threshold test flags are wanted.

- GENERATE_AEROSOL_FLAG (default no): Whether the aerosol flags are wanted.

- DO_POSTPROCESSING (default no): Whether the post processing to filter isolated pixels classified using AVHRR channel 3b shall be applied.

The CMa uses a number of static thresholds and threshold offsets, defined in the file threshold_offsets.cfg, with threshold_offsets_gac.cfg as an alternative. Altering these parameters which have been determined during algorithm tuning and validation, will strongly affect the quality of the CMa output. It is **not** recommended to modify these values. The file threshold_offsets.cfg should be used for running not-GAC data, and the file threshold_offsets_gac.cfg should be used for running GAC data.

## 4.2.3 Description of output

The content of the CMa consist of nine datasets, as described below. The aerosol flag is not fully developed yet.

**Main Output**

*Table 21: Cloud Mask*

| Number of the Class | Description/ Comments |
|---|---|
| 0 | Cloud-Free |
| 1 | Cloudy |
| Fill Value | No data/Undefined (separability problem) |

*Table 22: Cloud Mask extended*

| Number of the Class | Description/ Comments |
|---|---|
| 0 | Cloud-Free |
| 1 | Cloudy |
| 2 | Cloud contaminated |
| 3 | Snow/Ice |
| Fill Value | No data/Undefined (separability problem) |

**Threshold test flags**

Two 16 bit-lists to describe which test was successful: If a test is successful (cloudy) the test flags identifying the actual tests are set (the corresponding bit is activated). Thus all cloudy pixels will contain information on which tests were successful, both the decisive ones and any possible earlier tests where one or more of the features tested were close to its corresponding thresholds. Also the cloudfree pixels where one or more tests gave clear but were close (within safety margins) to cloudy threshold will have those testflags set (see description of the test sequence in section 4.1.2.10). Only the cloudfree pixels where no tests were successful, or close to succsessful, will have no test flags set at all.

*Table 23: Threshold test bits, part one*

| Bit number | Threshold test |
|---|---|
| 0 | T11Tsur |
| 1 | T11T3.7 |
| 2 | T3.7T12 |
| 3 | T11T12 |
| 4 | QR3.7R0.6 |
| 5 | R3.7 |
| 6 | R0.6 (or R0.9 if implemented) |
| 7 | T11_text |
| 8 | T3.7T12_text |
| 9 | R0.6_text |
| 10 | T11 |
| 11 | Tsur |
| 12 | Tsur-T950 |
| 13 | Probability for sunglint |
| 14 | PseudoR0.6 |
| 15 | QR1.6R0.6 |

*Table 24: Threshold test bits, part two*

| Bit number | Threshold test |
|---|---|

| Bit number | Threshold test |
|---|---|
| 0 | T85T11i |
| 1 | T85T11 |
| 2 | QR0.9R0.6 |
| 3 | Spatial homogeneity land |
| 4 | Spatial homogeneity sea |

**Status flags**

*Table 25: Status flag*

| Bit number | Description/Comment |
|---|---|
| 0 | Low level thermal inversion in NWP field |
| 1 | NWP data suspected low quality |
| 2 | Sea ice map is available |
| 3 | Sea ice, according to external map |
| 4 | No method for aerosol |
| 5 | Suspected heavy aerosol |

**Condition flags**

*Table 26  Conditions flag*

| Bit Number | Description |
|---|---|
| 0 | Pixel is out of swath or points to space |
| 1 and 2 | Defines the illumination condition:<br><br>0: N/A |

| **Bit Number** | **Description** |
| --- | --- |
| | 1: Night <br><br> 2: Day <br><br> 3: Twilight |
| 3 | Sunglint |
| 4 and 5 | Defines whether it is land or sea: <br><br> 0: N/A <br><br> 1: Land <br><br> 2: Sea <br><br> 3: Coast <br><br> This division in land/sea/coast is defined by the environmental variables SM_COASTALZONE_LIMIT (0 on default) and SM_LANDSEA_FRACTION_MAX (255 on default). See [RD.2.] for details. |
| 6 | High terrain |
| 7 | Rough terrain |
| 8 and 9 | Satellite input data status: <br><br> 0: N/A <br><br> 1: All satellite data are available <br><br> 2: At least one useful channel is missing <br><br> 3: At least one mandatory channel is missing |
| 10 and 11 | NWP input data status: <br><br> 0: N/A (not classified pixel or NWP data not used) <br><br> 1: All NWP data are available <br><br> 2: At least one useful NWP field is missing <br><br> 3: At least one mandatory NWP field is missing |
| 12 and 13 | Product input data status: <br><br> 0: N/A (not classified pixel or input product data not used) <br><br> 1: All product input data are available |

| Bit Number | Description |
|---|---|
|  | 2: At least one useful input product is missing <br><br> 3: At least one mandatory input product is missing |
| 14 and 15 | Auxiliary data status: <br><br> 0: N/A (not classified pixel or auxiliary data not used) <br><br> 1: All auxiliary data are available <br><br> 2: At least one useful auxiliary field is missing <br><br> 3: At least one mandatory auxiliary is missing |

**Quality flags**

*Table 27 Quality flag*

| Bit Number | Description |
|---|---|
| 0 | Pixel is NODATA |
| 1 | This bit is not used in PPS. It is a left over to keep the same bit numbers as GEO. |
| 2 | This bit is not used in PPS. It is a left over to keep the same bit numbers as GEO. |
| 3 to 5 | Retrieval quality: <br><br> 0: N/A (no data) <br><br> 1: Good <br><br> 2: Questionable <br><br> 3: Bad <br><br> 4: Interpolated/Reclassified |

**Aerosol flags**

The aerosol flag information is not yet fully developed. It is intended to detect excessive contents of aerosol due to volcanic eruptions, sand storms, or smoke from wild fires. In addition it might flag hot

spots from wild and industrial fires using the sensitive 3.7µm channel. Thus it will only detect extreme events, and not the sometimes common outbreaks of air with excessive aerosol contents due to industrial outlets.

For PPS v2016, the plan is to replace the aerosol flag. The new dataset will have fewer classes, but with higher quality in the information.

*Table 28: Aerosol bits*

| Bit number | Flag name | Description/Comment |
| --- | --- | --- |
| 0 | Not processed | Outside satellite swath, or over water bodies |
| 1 | Not contaminated | No detected contamination by dust clouds, volcanic ash plumes, fires (smoke from wild fires or hot spots from wild and industrial fires). |
| 2 | Smoke | Smoke from wild fires or volcanic ash plumes. |
| 3 | Dust clouds | Contamination by dust cloud. |
| 4 | Fire | Contamination by hot spots from wild and industrial fires. |
| 5 | Undefined | Not classified due to known separability problems. |

### 4.2.4 Visualisation

It is important to note that the PPS cloud and precipitation products first of all provide a digital analysis of the cloud and precipitation field, to be input to automatic mesoscale analysis or nowcasting schemes. Images may be derived and displayed to the forecaster but the products are not just images.

The CMa in particular is not the most obvious choice for image display at the forecaster's desk. The CMa rather is a base product being input to other SAF products like the CT, which is more suitable for image display. But if desired the CMa may be visualised, either directly using a hdfviewer and the cloud mask palette information available in the hdf5 file, or by using some dedicated image tool. Or looking at the png-images created by PPS; it comes in three versions: binary cloud mask, extended cloud mask and extended cloud mask with low-quality pixels marked.

Figure 5 show an example using the free image viewer *hdfview* available from the National Center for Supercomputing Applications (NCSA) in USA. Figure 6 shows the same example using a PPS products viewer developed at SMHI for algorithm development purposes. The SMHI viewer allows the synchronous display of both an instrument RGB and the cloud product. Pixel values (brightness temperature, reflectance, product value, flags etc.) may be shown under the mouse pointer.
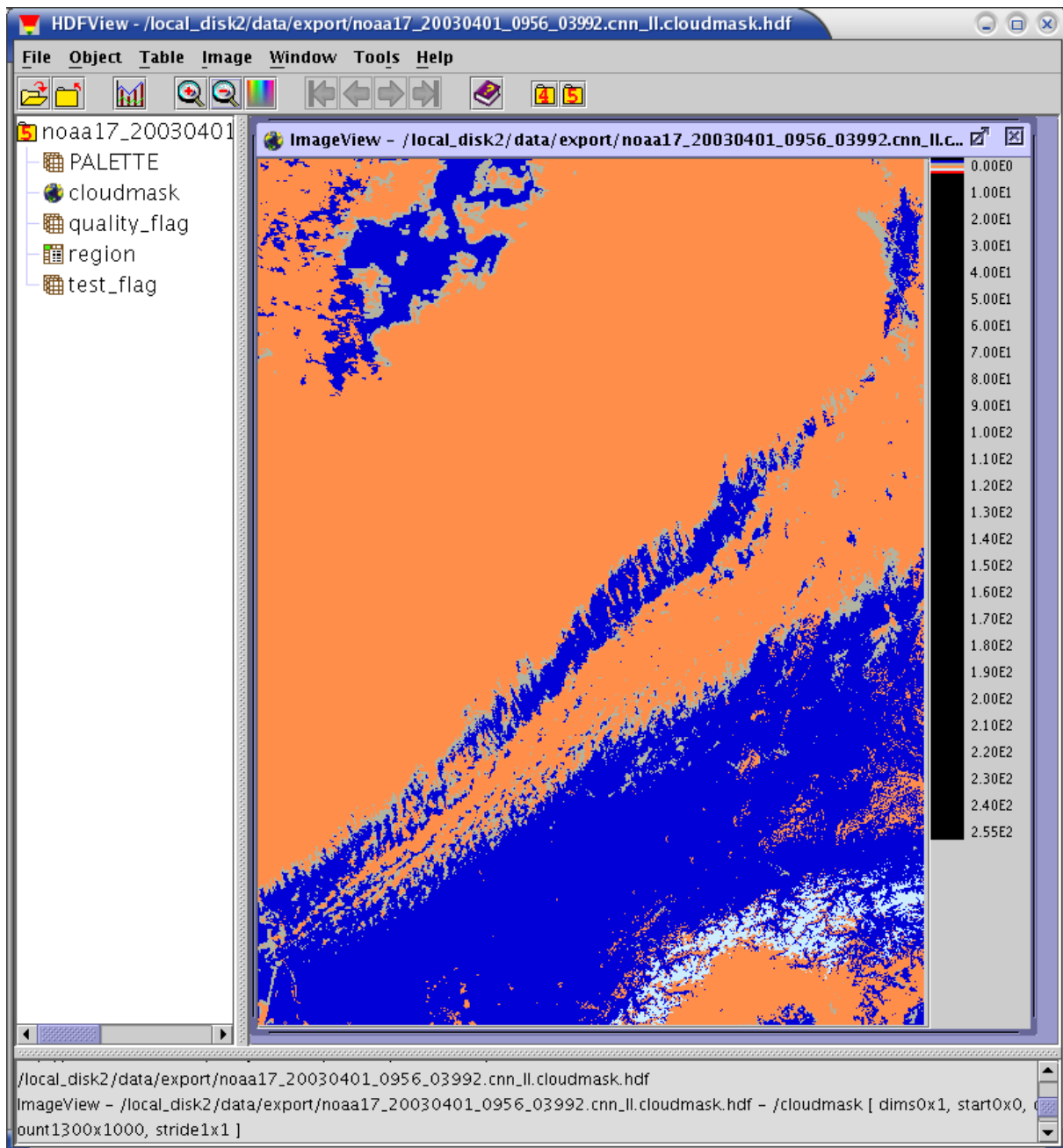
*Figure 5: An example of CMa image display using hdfview. A NOAA 17 scene over West Europe April 1, 2003, 9:56 UTC (orbit 3992).*
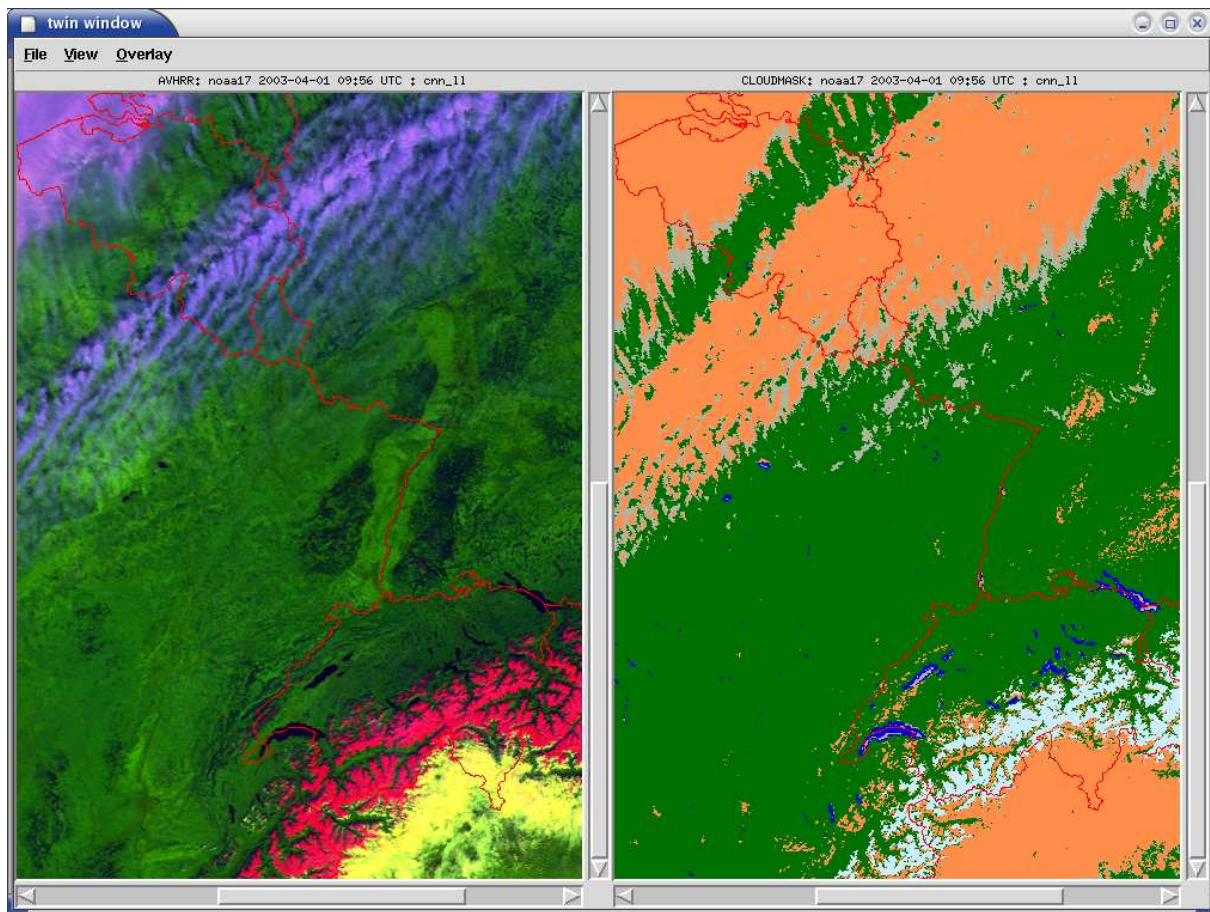
*Figure 6: Example of cloud mask image display using s dedicated PPS image viewer developed at SMHI. Same scene as shown in Figure 5. To the left a close up RGB image using 0.6µm, 1.6µm and 11µm channels is displayed and to the right the corresponding cloud mask using a land-sea mask to distinguish between sea and land.*

# ANNEX A. Summary SST algorithm descriptions and formalism

The algorithms below origins from the OSISAF team at Lannion, Pierre LeBorgne, et al., and is collected from various OSISAF documents including the official manual, and put together here for all satellites and using one and the same notation:

## 4.2.5 Formalism:

NLC = Non-Linear Complete algorithm

NL = Non-Linear algorithm

$T_{CLI}$ = climatologic SST, NWP t-skin for the climate

$S_\theta = 1/\cos(\theta) - 1$

### *Daytime: NLC*

$$SST = (a + b\, S_\theta)\ T_{11} + (c + d\, S_\theta + e T_{CLI})\ (T_{11} - T_{12}) + f + g\, S_\theta$$

### *Daytime: NL*

$$SST = a\, T_{11} + (b\, S_\theta + c T_{CLI})\ (T_{11} - T_{12}) + d + e\, S_\theta + corr$$

### *Nighttime: T37_1*

$$SST = (a + b\, S_\theta)\ T_{37} + (c + d\, S_\theta)\ (T_{11} - T_{12}) + e + f\, S_\theta + corr$$

The daytime NLC algorithm is slightly more accurate compared to the NL (personal communication Pierre LeBorgne, October 2013).

NB! **All temperatures expressed in Celcius**

## 4.2.6 Coefficients:

### 4.2.6.1 Metop-B

*Table 29 Metop-B SST algorithm coefficients*

|  | a | b | c | d | e | f | g | corr |
|---|---|---|---|---|---|---|---|---|
| **NLC** | 1.00400 | 0.00495 | 0.37766 | 0.59561 | 0.05609 | 0.61760 | 0.96388 | - |
| **NL** | 1.00244 | 0.68606 | 0.06692 | 0.85319 | 0.89201 | - | - | 0.0 |
| **T37_1** | 1.01432 | 0.02511 | 0.698846 | 0.35973 | 1.05387 | 0.99483 | - | 0.0 |

### 4.2.6.2  S-NPP

In Table 30 is described the coefficients of the non linear split window (NLC) and triple window (T37_1) algorithms for NPP/VIIRS, with all temperatures expressed in Celsius.

*Table 30 S-NPP SST algorithm coefficients*

|       | a       | b       | c       | d       | e       | f       | g       | corr |
|-------|---------|---------|---------|---------|---------|---------|---------|------|
| NLC   | 1.00055 | 0.00852 | 1.29073 | 0.0401  | 0.77930 | 1.05141 | 0.81520 | -    |
| T37_1 | 1.01612 | 0.01709 | 0.85154 | 0.36969 | 1.13960 | 0.82285 | -       | 0.0  |

### 4.2.6.3  Metop-A

*Table 31 Metop-A SST algorithm coefficients*

|        | a       | b       | c       | d       | e       | f       | corr |
|--------|---------|---------|---------|---------|---------|---------|------|
| **NL**    | 0.99052 | 0.06641 | 1.16321 | 1.26512 | 0.16400 | -       | 0.23 |
| **T37_1** | 1.01867 | 0.02109 | 0.68858 | 0.33056 | 1.02351 | 1.27303 | 0.13 |

### 4.2.6.4  NOAA-18

*Table 32 NOAA-18 SST algorithm coefficients*

|        | a       | b       | c       | d       | e       | f       | corr |
|--------|---------|---------|---------|---------|---------|---------|------|
| **NL**    | 0.97588 | 0.05905 | 0.95641 | 1.49882 | 0.28288 | -       | 0.0  |
| **T37_1** | 1.01477 | 0.01467 | 0.59010 | 0.30312 | 1.24160 | 1.2451 0 | 0.0 |

### 4.2.6.5  NOAA-19

*Table 33 NOAA-19 SST algorithm coefficients*

|  | a | b | c | d | e | f | corr |
|---|---|---|---|---|---|---|---|
| **NL** | 0.96832 | 0.05513 | 0.81105 | 1.5673 | 0.302 | - | 0.0 |
| **T37_1** | 1.01665 | 0.00851 | 0.54315 | 0.32588 | 1.01787 | 1.42468 | 0.0 |

### 4.2.6.6 NOAA-17 and older NOAA satellites

For NOAA-17 and older NOAA satellite we have no OSISAF algorithm coefficients. Therefore we use the coefficients for NOAA-18 and apply the SST based tests with larger and more cautious threshold offsets.

# ANNEX B. List of TBC, TBD, Open Points and Comments

| TBD/TBC | Section | Resp. | Comment |
|---|---|---|---|
|  |  |  |  |